AIAA 2003-4189

Compact Thermal Conductivity of Common Heat Sinks Used in Free and Forced Convection Studies

Kyle A. Brucker, Kyle T. Ressler and Joseph Majdalani
Marquette University
Milwaukee, WI 53233

36th AIAA Thermophysics Conference
23–26 June 2003
Orlando, FL

36th AIAA Thermophysics Conference
23-26 June 2003, Orlando, FL

AIAA 2003-4189

Compact Thermal Conductivity of Common Heat Sinks Used in Free and Forced Convection Studies

K. A. Brucker* K. T. Ressler† and J. Majdalani‡
Marquette University, Milwaukee, WI 53233

Growing trends towards miniaturization and improved functionality of chip packages have driven thermal analysts to explore innovative board designs that are cooled by multiple heat sinks. In view of pressing needs to reduce turnaround times, compact models have been developed in recent years for the purpose of decreasing the computational effort in system-level simulations of coupled heat sinks. This article focuses on the porous block model that is based on replacing an actual heat sink by the volume of fluid that once enveloped the fins. Thermal equivalence is achieved by increasing the thermal conductivity of the lumped fluid above the base plate until the thermal resistance of the actual heat sink is matched. The popularity of the porous block model can be attributed to its ability to approximate the three-dimensional isotherms established in a detailed heat sink. While previous investigations have focused on a numerically calculated effective thermal property of the compact model, this article presents a methodology leading to a closed-form analytical alternative. The explicit solutions that we provide are not only limited to the rectangular porous block models used in former studies. Rather, we extend the analysis to cover most fundamental body shapes and flow configurations under both free and forced convection modes. The exact or approximate formulations that we provide apply to most common Nusselt number correlations and obviate the need for initial guesswork or user-intervention to achieve convergence. They can be directly implemented in lieu of iterative algorithms to reproduce the equivalent thermal conductivity of a given heat sink.

Nomenclature

A_0 = $\mu C_p \mathrm{Gr}_L$
B_0 = a constant
C_p = constant pressure specific heat
g = acceleration due to gravity
Gr_L = Grashoff number, $g\beta\Delta TL^3\rho^2\mu^{-2}$
h = effective heat transfer coefficient
k = thermal conductivity
L = characteristic length
Pr = Prandtl number, $\mu C_p / k$
Ra_L = Rayleigh number, $g\beta\Delta TL^3\rho^2\mu^{-2}\mathrm{Pr}$
R_T = overall thermal resistance (junction-to-ambient)
T_b = bulk mean coolant temperature, $(T_i + T_o)/2$
T_f = film temperature, $(T_s + T_b)/2$
T_i = inlet coolant temperature
T_j = junction temperature
$T_{\max}$ = maximum surface temperature, T_j
T_o = outlet coolant temperature
T_s = surface temperature
T_∞ = ambient coolant temperature
U = overall heat transfer coefficient, $\dot{Q}/(A\Delta T)$

α = thermal diffusivity, $k/\rho C_p$
β = volumetric thermal expansion coefficient, $1/T_f$
ΔT = $T_s - T_b$
μ, ν = dynamic and kinematic viscosities
ρ = density

*Graduate Research Assistant. Presently at Cornell University, Ithaca, NY. Member AIAA.
†Graduate Research Assistant. Presently at Washington University in Saint Louis, Saint Louis, MO. Member AIAA.
‡Assistant Professor, Department of Mechanical and Industrial Engineering. Member AIAA.

I. Introduction

THE introduction of the microprocessor by Intel Corporation in 1971 has been accompanied by a rapid development of large-capacity memory chips whose packing density has increased from 10 million components in 1990 to 10 billion in 2000.[1] Excessive increases in very large-scale integration (VLSI) chip density have been further compounded by continued

miniaturization of chip carriers, multichip packages, and printed circuit boards (PCBs). Pressing demands for size reduction and improved performance of electronic equipment have resulted in the development of high-power components dissipating significant amounts of heat per unit volume. Since the failure rate of electronic components increases exponentially with operating temperatures, the need for quick thermal-control remedies has gradually become a chief concern in the design and reliability assessment of electronic equipment. This is especially true of electronic enclosures, cabinets, or cases, in which several hundred PCBs, racks, brackets, switches, lights, connectors, control interfaces, and other peripherals have to be packaged. In addition to the challenging task of determining proper cooling loads and solutions, the thermal engineering team is confronted with the need to produce a well-designed housing that provides easy access for replacing failed components, minimizing downtime, and facilitating maintainability.

A number of exotic cooling methods are available today and these are summarized in a survey by Bar-Cohen and Kraus.[2] Generally, these methods rely on a variety of concepts including, but not limited to, free and forced air and liquid cooling, air impingement, liquid immersion, thermoelectric cooling, and heat pipes. So far it appears that the use of heat sinks has been the most widely adopted vehicle for heat removal in populated PCBs. Historically, these compact heat exchangers have been introduced by Kays and London[3] and then carefully explored by Tuckerman and Pease.[4] They continue to receive favour in the works of Goldberg,[5] Sasaki and Kishimoto,[6] Hwang, Turlik and Reisman,[7] Nayak *et al.*,[8] Phillips,[9] Gavali *et al*.,[10] Butterbaugh and Kang,[11] Visser and Gauche,[12] and many others.[13]

Heat sinks can be operated under free or forced convective modes depending on the cooling load requirement. Free convection remains the most desirable and deliberate form of cooling being quiet, reliable, simple, and, most of all, free. Nevertheless, thermally-induced buoyancy currents have not always been adequate in cooling high-density chip packages. Thermal-enhancement techniques are often needed to lower the resistance of a heat sink by increasing its effective surface area beyond the optimal value granted by free convection. To do so, higher fin densities per base plate are needed, and these require better air circulation than is possible naturally. The push or pull air cooling approach is usually resorted to and this is accomplished through the use of intake and/or exhaust fans.[14]

In its early development, heat sink implementation was slow and expensive as it mostly relied on a blend of theory[13,14] and experimentation.[15-17] With the dramatic growth in computer technology, this focus has shifted to the use of computational fluid dynamics (CFD).[10-14] The latter has appeared to offer a fast and reliable alternative, especially when applied to small-scale assemblies.

The adoption of CFD as the method of choice has not been without challenges. Despite modern leaps in processor speed, the discretization demands in modeling increasingly more sophisticated arrays of microchips seem to be in constant catch-up mode with available computer resources. This is especially true when considering the significant number of boards, pads, high frequency interconnects, and space constraints in designing populated assemblies of multichip modules (MCMs). While a detailed CFD treatment may be practical in analyzing small subassemblies, it clearly becomes overly time-consuming and unaffordable in many applications of real concern.

In order to better cope with the accelerated product development cycles confronting thermal engineers, lumped, coarse, or compact heat sink models have been proposed in recent years. Examples abound and one may cite the forced convection simulations by Bar-Cohen, Elperin and Eliasi,[18] Krueger and Bar-Cohen,[19] Culham, Yovanovich and Lee,[20,21] Linton and Agonafer,[22] Butterbaugh and Kang,[11] Visser and Gauche,[12] Patel and Belady,[23,24] Kim and Lee,[25] and Narasimhan and Kusha.[26] The same principle has been extended to physical settings involving free convection by Narasimhan and Majdalani.[27,28] All in all, the main idea has been to replace the heat sink with a simpler model that is capable of providing the same thermal and fluid resistance properties exhibited by the actual device. For added convenience, compact modeling has relied on known empirical correlations for predicting flow attributes. Based on the thermal resistance concept, three techniques have been employed so far. These are the 'boundary condition independent BC-model,' the 'flat plate boundary-layer model,' and the 'porous block' or 'volume resistance model.'

The BC model is based on the notion that a chip package can be characterized by a limited number of well-chosen thermal resistances. At the outset, the model's level of complexity and detail can vary significantly depending on the thermal design requirements. In simple models, a single lumped thermal capacitance is used for each distinct component. In more sophisticated representations, multiple resistors, nodes and shunts can be used in representing top, bottom, side and lead areas that provide passage to heat. The purpose is for the resulting thermal network to provide acceptable approximations

for chip temperatures and flow contours. While the original name and formulation must be attributed to Bar-Cohen, Elperin and Eliasi,[18] the BC-approach seems to have evolved from the works of Andrews, Mahalingam and Berg,[29] Andrews,[30] and Mahalingam.[31] Since its inception, it has been used by Gautier,[32] Le Jannou and Huon,[33] Lemczyk *et al.,*[34,35] Lasance, Vinke and Rosten,[36] and several others.

The flat plate model is also based on an equivalent thermal resistance concept that has been thoroughly described by Culham, Yovanovich and Lee.[21] In short, it is implemented by determining the overall thermal resistance R_T from the heat sink and then assigning it either to the base plate, the extended base plate, the raised fin, or the raised fin with base plate assembly.

Instead of assigning the effective thermal resistance to a two-dimensional surface, the porous block model is different in that it distributes R_T uniformly over the three-dimensional volume of fluid that was once occupied by the fins. Following Patel and Belady[23] or Narasimhan and Majdalani,[28] reducing the thermal resistance of the volume of fluid above the base plate can be accomplished by artificially increasing its thermal conductivity. An effective thermal conductivity k_e can thus be determined and assigned to the volume of fluid in an attempt to match the required thermal resistance R_T. Being capable of reproducing three-dimensional temperature maps and heat transfer pathways in an actual heat sink, this approach has been recently adopted by Narasimhan, Bar-Cohen and Nair.[37]

In forced convection models, an equivalent pressure loss coefficient needs to be additionally determined in order to account for the flow resistance across the finned space. This problem is further exacerbated by the 'flow bypass effect' caused by the presence of complicated flow pathways through and around the heat sink. In practice, this effect is often manifested by the formation of horseshoe vortices around the heat sink. These vortices are attributed to the increased hydraulic resistance resulting from the narrowing down of flow passages. The higher flow impedance causes the cooling fluid to escape through the side or top clearance above the fin tips following the path of least resistance (Kim and Lee[25]). Inevitably, the flow bypass effect becomes significant in unducted heat sinks where no shroud is available to suppress the flow bypass. Studies aiming at improving the prediction of hydraulic loss coefficients include those by Souza, Mendes and Santos,[15] Vogel,[16] Wirtz, Chen and Zhou,[17] Butterbaugh and Kang,[11] Patel and Belady,[23] Teertstra, Yovanovich and Culham,[38] and Narasimhan, Bar-Cohen and Nair.[39] In the free convection models examined by Narasimhan and Majdalani,[27,28] calculating the small pressure loss in the detailed heat sink simulation has posed a lesser challenge. Conversely, determining the effective thermal conductivity has been considered more difficult due to the increased algebraic complexity of empirical correlations for buoyancy-driven flows.

It should be noted that, throughout these studies, standard heat transfer correlations have been used in calculating equivalent thermal properties. This is especially true of porous block models that require evaluating the effective thermal conductivity k_e of the detailed heat sink. In previous investigations, k_e had to be determined numerically from standard heat transfer correlations (e.g., those by Churchill and Chu[40]) for laminar and turbulent flow over a flat plate. Furthermore, applications have been limited to tetrahedral heat sinks that give rise to rectangular porous blocks. In reality, however, electronic cooling applications involve a diverse mix of geometric configurations, sizes, shapes, and orientations. In cylindrical heat sinks, for example, base plates have circular cross-sections. Since non-rectangular heat sinks and base plates have not been considered in compact heat sink modeling, it is the intent of this article to present closed-form solutions for the effective thermal conductivity of different geometric configurations that are encountered in industrial units. Our methodology will be based on either exact or asymptotic solutions for those cases in which k_e has been iteratively determined in previous studies. It is hoped that the direct solutions for k_e will obviate the need for numerical root solving, bracketing, and user-intervention. Considering that the operating environment for compact heat sinks is not known beforehand, the explicit solutions that we seek for k_e will be presented in a general form to facilitate portability. After covering the widely used rectangular geometry, our approach will be extended to other physical configurations that constitute the building blocks of complex heat sinks. In the meantime, our analysis will target both free and forced convection modes under laminar, turbulent and combined flow regimes

II. The Equivalent Thermal Resistance

In order to ensure that the thermal resistance of a compact model matches that of a detailed heat sink, a few steps must be carried out before the effective thermal conductivity of the corresponding porous block can be determined. The key is to obtain the overall heat transfer coefficient characterizing the actual heat sink. These steps are described in several articles including those by Patel and Belady,[23] Kim and Lee,[25] and Narasimhan and Majdalani.[28] They are summarized here for the sake of clarity.

The key step consists of calculating the overall thermal resistance R_T of the actual heat sink. This

parameter is an important figure-of-merit used in characterizing the efficacy of competing chip layouts (Lasance, Vinke and Rosten[36]). It is also known as the junction-to-ambient or junction-to-coolant thermal resistance. For a constant heat dissipation rate $\dot{Q}$, it is calculated from $R_T = \Delta T / \dot{Q}$. The temperature excess $\Delta T = T_{\max} - T_b$ is based on the maximum surface temperature $T_{\max}$ and the coolant temperature T_b. In free convection studies, T_b can be equated to the ambient temperature T_∞. To find R_T, $T_{\max}$ is conveniently acquired from a detailed heat sink solution. It can also be obtained from experimental measurements or theoretical relations available for a similar heat sink. This value is determined only once for a given cooling load $\dot{Q}$. Thus, as a large-scale system is being developed, only compact properties are calculated and allocated to each heat sink. This allocation is usually based on preliminary heat sink sizings that result in a simple model. If changes are later needed, only equivalent resistances are altered, without changing the physical model or its mesh resolution. As the mesh remains unmodified, re-initialization is eliminated, and convergence is faster achieved. A flowchart describing the efficacy of compact models in reducing turnaround times is provided by Patel and Belady.[23] Surely a detailed heat sink simulation is greatly expedited when a validated numerical model is supplied by the vendor (cf. Bar-Cohen, Elperin and Eliasi[18]).

Under forced convection conditions, the temperature excess ΔT can be made more sensitive by basing it on the log-mean temperature difference (LMTD) suggested by Kraus and Bar-Cohen.[41] This value can be calculated from $\Delta T = (T_o - T_i)/\ln[(T_s - T_i)/(T_s - T_o)]$, where T_i and T_o represent the inlet and outlet temperatures directly upstream and downstream of the heat sink. The outlet temperature can be obtained from the coolant flowrate $\dot{m}$, and specific heat C_p, via $T_o = T_i + \dot{Q}/(\dot{m}C_p)$.

Regardless of the technique used in determining R_T, the next step consists of evaluating the overall heat transfer coefficient U between the base plate and surrounding fluid. This is readily obtainable from $U = (R_T A_b)^{-1}$ where A_b is the surface area of the base plate. The use of an overall heat transfer coefficient in the porous block model constitutes a minor departure from the flat plate boundary-layer model where an effective conductance h_e is employed (see Culham, Yovanovich and Lee,[21] Gavali *et al.*[10] and Vogel[16]). In the base plate surface model, for example, the Nusselt number correlation for flow over a vertical plate is used to calculate the heat transfer coefficient h_{hs} from an actual heat sink with total surface area A_{hs}. Recalling that the thermal resistance at the base plate is $(h_e A_b)^{-1}$, the equivalent h_e is then calculated by setting $h_e A_b = A_{hs} h_{hs}$. If $T_{\max}$ estimated by the flat plate model is made to coincide with the maximum surface temperature obtained numerically, both models will then possess the same thermal resistance, $R_T = (h_e A_b)^{-1}$. Consequently, one would have $U = h_e$. The symbol U instead of h_e is presently used because the thermal resistance $R_T = (UA_b)^{-1}$ combines, in most models, the effects of convection and radiation. This is due to both modes of heat transfer being accounted for in the detailed CFD simulations used by most investigators in the process of evaluating R_T. This is also true of laboratory measurements in which radiation effects are implicitly captured.

Once U is determined, one can proceed to the third and final step of calculating the effective thermal conductivity of the compact model. This step involves substituting U for h_e in an accepted form of the Nusselt number correlation for the specific case at hand. In free convection studies, the archetypical example consists of a laminar buoyancy-driven flow along a vertically oriented base plate. Since the presence of fins is suppressed in the compact representation, the empirical correlation by Churchill and Chu[42] for flow over a vertical plate becomes appropriate. Using standard descriptors, one may write

$$\mathrm{Nu}_L = UL/k_e = 0.68 + 0.67\mathrm{Ra}_L^{1/4} \times \left[1 + \left(0.492/\mathrm{Pr}\right)^{9/16}\right]^{-4/9} \quad (1)$$

where the Rayleigh number is given by

$$\mathrm{Ra}_L = g\beta\Delta TL^3/(\nu\alpha) \quad (2)$$

Customarily, the isothermal surface condition $T_s = T_{\max}$ is used. This assumption is adopted by most thermal analysts to ensure design safety for given cooling load and geometric constraints. In the foregoing relation, all properties are either known or prescribed by the cooling requirement except for k_e. One must also recognize that this effective thermal conductivity is not that of the coolant at film temperature. Rather, it is an artificially adjusted value that must be assigned to the parallelepiped of fluid above the base plate that once enveloped the fins. Hence, by properly increasing the thermal conductivity of the block of fluid above the base plate, its thermal resistance is reduced in a manner to reproduce the same three-dimensional thermal resistance associated with the actually finned heat sink. According to the porous block methodology, the thermal conductivity of the coolant is locally increased while entering the 'finned' space above the base plate. This is done for the purpose of promoting the same overall heat transfer coefficient characterizing the detailed heat sink. The reduced thermal resistance above the base can thus produce gradual temperature

variations that mimic the three-dimensional temperature maps projected by a detailed CFD analysis. Clearly, the porous block approach can be seen to be different from the flat plate model in which the temperature drop $T_{\max} - T_b$ is applied across the thin base plate.

In past studies, an iterative approach has been resorted to every time to calculate k_e from Eq. (1) by solving the transcendental expression

$$0 = -\frac{UL}{k_e} + 0.68 + \frac{0.67(\rho C_p g \beta \Delta T L^3)^{1/4}}{(\nu k_e)^{1/4}\left[1+\left(0.492 k_e\right)^{9/16}\left(\mu C_p\right)^{-9/16}\right]^{4/9}} \qquad (3)$$

In the current work, a direct asymptotic solution for k_e will be developed such that the need for numerical iterations is eliminated. The same approach will also be applied to other fundamental configurations whose effective thermal conductivities have not been evaluated yet.

III. General Free Convection

The technical literature is filled with empirical correlations aimed at predicting free convection heat transfer from an isothermal body to a quiescent fluid. These correlations vary in complexity from the simplest form, $\mathrm{Nu}_L = C\mathrm{Ra}_L^m$, to the more general form, $\mathrm{Nu}_L = a_0 + a_1\mathrm{Ra}_L^m$.[40] The latter extends over a wider range of Rayleigh numbers and contains two constants a_0 and a_1 that depend on both geometry and flow regime. The leading-order constant a_0 is added to account for thermal diffusion effects as they become increasingly more important at smaller values of Ra_L. Based on boundary-layer theory, m is taken to be $\frac{1}{4}$ or $\frac{1}{3}$ depending on whether the flow is laminar or turbulent.[1] When the cooling fluid is not air, the Rayleigh number is often multiplied by a universal Prandtl number function exhibiting the familiar form

$$F(\mathrm{Pr}) = \left[1+\left(a_2/\mathrm{Pr}\right)^n\right]^r = \left[1+\left(0.492/\mathrm{Pr}\right)^{9/16}\right]^{-16/9} \qquad (4)$$

In Eq. (4) the right hand side gives the form of F for laminar flow over a flat plate (see Churchill and Churchill[43]). For the sake of generality, this correction factor can be readily incorporated by writing

$$\mathrm{Nu}_L = a_0 + a_1\mathrm{Ra}_L^m\left[1+\left(a_2/\mathrm{Pr}\right)^n\right]^{mr} \qquad (5)$$

The resulting equation can be used to simultaneously represent free convection over a vertical plate, a horizontal, vertical or inclined cylinder, a cube in several orientations, a sphere, a bisphere, a prolate spheroid and an oblate spheroid. The corresponding constants a_0, a_1, a_2, m, n and p are posted in Table 1.

In addition to Eq. (5) a particularly useful form proposed by Churchill and Chu[40] stretches over the entire range of Rayleigh numbers. Using standard nomenclature, this correlation can be expressed by

$$\mathrm{Nu}_L = \left\{a_0 + a_1\mathrm{Ra}_L^{m/q}\left[1+\left(a_2/\mathrm{Pr}\right)^n\right]^{mr/q}\right\}^q \qquad (6)$$

Equation (6) is appropriate of vertical flat plates, inclined flat plates, vertical or horizontal cylinders, vertical cones, spheres, inclined disks, and spherelike surfaces. Corresponding constants in Eq. (6) are listed in Table 1 as well.

In what follows, we hope to present the explicit solution for k_e depending on the equation type. By going from simple to complex, we not only hope to cover a broad range of correlations, but also provide sufficient examples to establish a systematic methodology. Such methodology could later be used to derive k_e in those physical settings that are not covered here.

IV. Exact k_e for Free Convection

For a correlation of the type $\mathrm{Nu}_L = C\mathrm{Ra}_L^m$, an exact solution k_e is available directly from

$$k_e = \mathrm{Gr}_L\mu Cp[UL/(C\mathrm{Gr}_L\mu Cp)]^{1/(1-m)} \qquad (7)$$

However, when $\mathrm{Nu}_L = a_0 + a_1\mathrm{Ra}_L^m$, a general solution must be obtained by solving for the meaningful root of

$$a_0 k_e + a_1(\mathrm{Gr}_L\mu C_p)^m k_e^{1-m} - UL = 0 \qquad (8)$$

Two special cases arise depending on whether the flow under consideration is laminar ($m = 1/3$) or turbulent ($m = 1/4$). For laminar flow, Eq. (8) yields the cubic polynomial

$$k_e^3 + (a_1/a_0)^3\mathrm{Gr}_L\mu C_p k_e^2 - (UL/a_0)^3 = 0\,. \qquad (9)$$

In this instance, the physical root k_e may be determined using Cardano's method[44] Two possibilities emerge depending on the sign of Cardano's discriminant,

$$\Delta = (UL/a_0)^6 - \left[(a_1/a_0)^3\mathrm{Gr}_L\mu C_P\right]^3(UL/a_0)^3\,. \qquad (10)$$

When $\Delta < 0$, a trigonometric root emerges. This is

$$k_e = \tfrac{1}{3}b_0\left(2\cos\theta - 1\right)$$

$$\theta \equiv \tfrac{1}{3}\cos^{-1}\left(\tfrac{27}{2}b_1 b_0^{-3} - 1\right),$$

$$b_0 \equiv \left(a_1/a_0\right)^3\mathrm{Gr}_L\mu C_P\,,\; b_1 \equiv \left(UL/a_0\right)^3 \qquad (11)$$

Table 1 Effective thermal conductivity of common geometric shapes under free convection

	Description	Free convection correlation	Effective thermal conductivity
1	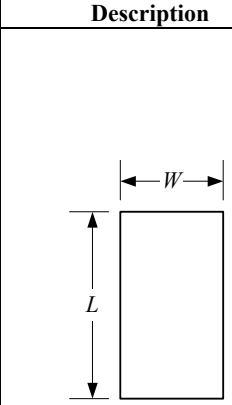 vertical plate	$\mathrm{Nu}_L = 0.68 + \dfrac{0.67\mathrm{Ra}_L^{1/4}}{\left(1+0.671\mathrm{Pr}^{-9/16}\right)^{4/9}}$ laminar, Churchill and Chu[40]	$k_e \rightarrow$ Eq. (36), $10^0 \le \mathrm{Ra}_L \le 10^9$ $(m,n,p) = (\frac{1}{4}, \frac{9}{16}, -\frac{4}{9})$, $a_i = (0.68, 0.67, 0.492)$ $s_i = (2\times10^{-7}, -2\times10^{-5}, 0.0012, -0.0465, 1.0311)$
2		$\mathrm{Nu}_L = \left[0.825 + \dfrac{0.387\mathrm{Ra}_L^{1/6}}{\left(1+0.671\mathrm{Pr}^{-9/16}\right)^{8/27}}\right]^2$ laminar or turbulent Churchill and Chu[40]	$k_e \rightarrow$ Eq. (57), $10^0 \le \mathrm{Ra}_L \le 10^{13}$ $a_i = (0.825, 0.387, 0.492)$ $s_i = (2\times10^{-7}, -2\times10^{-5}, 0.0012, -0.0463, 1.0304)$
3		$\mathrm{Nu}_L = 0.59\mathrm{Ra}_L^{1/4}$ laminar, McAdams[45]	$k_e = 2.03\sqrt[3]{(UL)^4/(\mathrm{Gr}_L\mu C_P)}$, $10^4 \le \mathrm{Ra}_L \le 10^9$
4		$\mathrm{Nu}_L = 0.1\mathrm{Ra}_L^{1/3}$ turbulent, Warner and Arpaci[46]	$k_e = 31.62\sqrt{(UL)^3/(\mathrm{Gr}_L\mu C_P)}$, $10^9 \le \mathrm{Ra}_L \le 10^{13}$
5		$\mathrm{Nu}_L = 0.021\mathrm{Ra}_L^{2/5}$ turbulent, Eckert and Jackson[47]	$k_e = 1.6\times10^{-3}\sqrt{(UL)^5/(\mathrm{Gr}_L\mu C_P)^2}$ $10^9 \le \mathrm{Ra}_L \le 10^{13}$
6	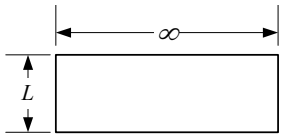 horizontal plate $L = \dfrac{A}{P}$	$\mathrm{Nu}_L = 0.27\mathrm{Ra}_L^{1/4}$, hot side down Lloyd and Moran[48]	$k_e = 62.9\sqrt[3]{(UL)^4/(\mathrm{Gr}_L\mu C_P)}$, $10^5 < \mathrm{Ra}_L < 10^{11}$
7		$\mathrm{Nu}_L = 0.54\mathrm{Ra}_L^{1/4}$, hot side up laminar, Lloyd and Moran[48]	$k_e = 2.274\sqrt[3]{(UL)^4/(Gr_L\mu C_P)}$, $10^4 \le \mathrm{Ra}_L \le 10^7$
8		$\mathrm{Nu}_L = 0.15\mathrm{Ra}_L^{1/3}$, hot side up turbulent, Lloyd and Moran[48]	$k_e = 0.0581\sqrt{(UL)^3/(Gr_L\mu C_P)}$, $10^7 \le \mathrm{Ra}_L \le 10^{10}$
9	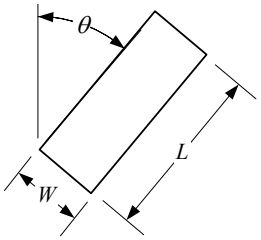 inclined pate with heated surface facing downward	$\mathrm{Nu}_L = 0.56\left(\mathrm{Ra}_L\cos\theta\right)^{1/4}$ $T_f \rightarrow T_e = T_s - 0.25(T_s - T_\infty)$ $\beta = 1/T_\beta$, $T_\beta = T_\infty + 0.50(T_s - T_\infty)$ laminar, Fujii and Imura[49]	$k_e = 2.166\sqrt[3]{(UL)^4/(\mathrm{Gr}_L\mu C_p\cos\theta)}$ $10^5 \le \mathrm{Ra}_L\cos\theta \le 10^{11}$, $0° \le \cos\theta \le 89°$
10		$\mathrm{Nu}_L = \left[0.825 + \dfrac{0.387\mathrm{Ra}_L^{1/6}}{\left(1+0.671\mathrm{Pr}^{-9/16}\right)^{8/27}}\right]^2$ laminar or turbulent, Churchill[50]	$k_e \rightarrow$ Eq. (57), $\forall\mathrm{Ra}_L$, $g \rightarrow g\cos\theta$, $\theta \le 60°$ $a_i = (0.825, 0.387, 0.492)$ $s_i = (2\times10^{-7}, -2\times10^{-5}, 0.0012, -0.0463, 1.0304)$
11	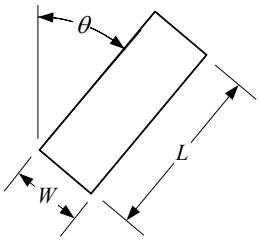 inclined plate with heated surface facing upward	$\mathrm{Nu}_L = 0.17\left(\mathrm{Gr}_L^*\mathrm{Pr}\right)^{1/4}$ $\mathrm{Gr}_L^* = g\beta UL^4\cos\theta/(k\nu^2)$	$k_e = \left\{[0.17\left(\mathrm{g}\beta\mu\mathrm{C}_P UL^4\cos\theta/\nu^2\right)^{1/4}]/(UL)\right\}^2$ $10^{10} < \mathrm{Gr}_L^*\mathrm{Pr} < 10^{15}$

	Description	Free convection correlation	Effective thermal conductivity
12	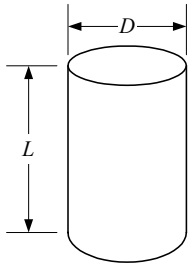 **vertical cylinder**	$\mathrm{Nu}_L = 0.68 + \dfrac{0.67\mathrm{Ra}_L^{1/4}}{\left(1+0.671\mathrm{Pr}^{-9/16}\right)^{4/9}}$ laminar, Churchill and Chu[40]	$k_e \rightarrow$ Eq. (36), $10^0 \le \mathrm{Ra}_L \le 10^9$ $D/L \ge 35/\mathrm{Gr}_L^{1/4}$ $a_i = (0.68, 0.67, 0.492)$, $(m,n,p) = (\frac{1}{4}, \frac{9}{16}, -\frac{4}{9})$ $s_i = (2\times10^{-7}, -2\times10^{-5}, 0.0012, -0.0465, 1.0311)$
13		$\mathrm{Nu}_L = 3.444 + \dfrac{0.645\mathrm{Ra}_L^{1/4}}{\left(1+0.671\mathrm{Pr}^{-9/16}\right)^{4/9}}$ laminar, Yovanovich[51]	$k_e \rightarrow$ Eq. (36), $0 \le \mathrm{Ra}_L \le 10^8$, $L = A_w^{1/2}$ $a_i = (3.444, 0.645, 0.492)$, $(m,n,p) = (\frac{1}{4}, \frac{9}{16}, -\frac{4}{9})$ $s_i = (2\times10^{-7}, -2\times10^{-5}, 0.0012, -0.0465, 1.0311)$
14		$\mathrm{Nu}_L = \left[0.825 + \dfrac{0.387\mathrm{Ra}_L^{1/6}}{\left(1+0.671\mathrm{Pr}^{-9/16}\right)^{8/27}}\right]^2$ laminar or turbulent, Churchill[50]	$k_e \rightarrow$ Eq. (57), $\forall \mathrm{Ra}_L$, $D/L \ge 35/\mathrm{Gr}_L^{1/4}$ $a_i = (0.825, 0.387, 0.492)$ $s_i = (2\times10^{-7}, -2\times10^{-5}, 0.0012, -0.0463, 1.0304)$
15		$\mathrm{Nu}_L = 0.53\mathrm{Ra}_L^{1/4}$ laminar, McAdams[45]	$k_e = 2.02\sqrt[3]{(UL)^4/(\mathrm{Gr}_L\mu C_P)}$, $10^4 \le \mathrm{Ra}_L \le 10^9$
16		$\mathrm{Nu}_L = 0.1\mathrm{Ra}_L^{1/3}$ turbulent, Warner and Arpaci[46]	$k_e = 31.62\sqrt{(UL)^3/(\mathrm{Gr}_L\mu C_P)}$, $10^9 \le \mathrm{Ra}_L \le 10^{13}$ $D/L \ge 35/\mathrm{Gr}_L^{1/4}$
17		$\mathrm{Nu}_L = 3.444 + \dfrac{0.683\mathrm{Ra}_L^{1/4}}{\left(1+0.671\mathrm{Pr}^{-9/16}\right)^{4/9}}$ laminar, Yovanovich[51]	$k_e \rightarrow$ Eq. (36), $10^0 \le \mathrm{Ra}_L \le 10^9$, $L = \frac{1}{2}D\pi^{1/2}$ $a_i = (3.444, 0.683, 0.492)$, $(m,n,p) = (\frac{1}{4}, \frac{9}{16}, -\frac{4}{9})$ $s_i = (2\times10^{-7}, -2\times10^{-5}, 0.0012, -0.0465, 1.0311)$
18	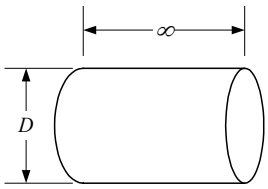 **horizontal cylinder**	$\mathrm{Nu}_D = 0.36 + \dfrac{0.518\mathrm{Ra}_D^{1/4}}{\left(1+0.721\mathrm{Pr}^{-9/16}\right)^{4/9}}$ laminar, Churchill and Chu[52]	$k_e \rightarrow$ Eq. (37), $10^{-6} < \mathrm{Ra}_D < 10^9$ $L = D$ $a_i = (0.36, 0.518, 0.559)$, $(m,n,p) = (\frac{1}{4}, \frac{9}{16}, -\frac{4}{9})$ $s_i = (2\times10^{-7}, -2\times10^{-5}, 0.0012, -0.0465, 1.0311)$
19		$\mathrm{Nu}_D = \left[0.60 + \dfrac{0.387\mathrm{Ra}_D^{1/6}}{\left(1+0.721\mathrm{Pr}^{-9/16}\right)^{8/27}}\right]^2$ turbulent, Churchill and Chu[52]	$k_e \rightarrow$ Eq. (57), $\mathrm{Ra}_D \ge 10^9$, $L = D$ $a_i = (0.60, 0.387, 0.559)$ $s_i = (2\times10^{-6}, -0.0001, 0.0042, -0.087, 1.0298)$
20		$\mathrm{Nu}_D = 0.675\mathrm{Ra}_D^{0.058}$, $10^{-10} \le \mathrm{Ra}_D \le 10^{-2}$ $\mathrm{Nu}_D = 1.02\mathrm{Ra}_D^{0.148}$, $10^{-2} < \mathrm{Ra}_D \le 10^2$ $\mathrm{Nu}_D = 0.85\mathrm{Ra}_D^{0.188}$, $10^2 < \mathrm{Ra}_D \le 10^4$ $\mathrm{Nu}_D = 0.48\mathrm{Ra}_D^{1/4}$, $10^4 < \mathrm{Ra}_D \le 10^7$ $\mathrm{Nu}_D = 0.125\mathrm{Ra}_D^{1/3}$, $10^7 < \mathrm{Ra}_D \le 10^{12}$ Morgan[53]	$k_e = \{UL/[0.675(Gr_L\mu C_P)^{0.058}\}^{1.062}$ $k_e = \{UL/[1.02(Gr_L\mu C_P)^{0.148}]\}^{1.174}$ $k_e = \{UL/[0.85(Gr_L\mu C_P)^{0.188}]\}^{1.234}$ $k_e = \{UL/[0.48(Gr_L\mu C_P)^{1/4}]\}^{4/3}$ $k_e = \{UL/[0.125(Gr_L\mu C_P)^{1/3}]\}^{3/2}$

	Description	Free convection correlation	Effective thermal conductivity
21	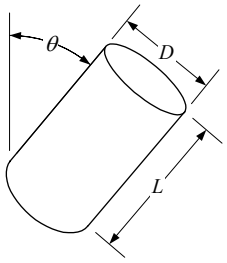 **inclined cylinder**	$\mathrm{Nu}_L = \left[2.9 - 2.32(\sin\theta)^{0.8}\right] \times \mathrm{Gr}_D^{-1/12}\left(\mathrm{Gr}_L\,\mathrm{Pr}\right)^{0.1\sin\theta+0.25}$ $\left(\mathrm{Gr}_L\,\mathrm{Pr}\right)_{\mathrm{cr}} = 2.6\times10^9 + 1.1\times10^9\tan\theta$ laminar, Al-Arabi[54]	$k_e = \left[ULB^{-1}\left(Gr_L\mu C_p\right)^{-1/4-0.1\sin\theta}\right]^{1.75-0.1\sin\theta}$ $B = 2.9 - 2.32\left(\sin\theta\right)^{0.8}\mathrm{Gr}^{-1/12}$ $9.88\times10^7 \le \mathrm{Gr}_L\,\mathrm{Pr} \le \left(\mathrm{Gr}_L\,\mathrm{Pr}\right)_{\mathrm{cr}}$ $1.08\times10^4 \le \mathrm{Gr}_D\,\mathrm{Pr} \le 6.9\times10^5$
22		$\mathrm{Nu}_L = \left[0.47 - 0.11(\sin\theta)^{0.8}\right] \times \mathrm{Gr}_D^{-1/12}\left(\mathrm{Gr}_L\,\mathrm{Pr}\right)^{1/3}$ $\left(\mathrm{Gr}_L\,\mathrm{Pr}\right)_{\mathrm{cr}} = 2.6\times10^9 + 1.1\times10^9\tan\theta$ turbulent, Al-Arabi[54]	$k_e = \sqrt{\dfrac{(UL)^3\mathrm{Gr}_L^{-3/4}}{[0.47 - 0.11(\sin\theta)^{0.8}]\mu C_P}}$ $\left(\mathrm{Gr}_L\,\mathrm{Pr}\right)_{\mathrm{cr}} \le \mathrm{Gr}_L\,\mathrm{Pr} \le 2.95\times10^{10}$ $1.08\times10^4 \le \mathrm{Gr}_D\,\mathrm{Pr} \le 6.9\times10^5$
23		$\mathrm{Nu}_L = 3.444 + \dfrac{0.673\mathrm{Ra}_L^{1/4}}{\left(1+0.671\mathrm{Pr}^{-9/16}\right)^{4/9}}$ $\theta = 45°$, laminar, Yovanovich[51]	$k_e \rightarrow$ Eq. (36), $10^0 \le \mathrm{Ra}_L \le 10^9$, $L = A_w^{1/2}$ $a_i = (3.444, 0.673, 0.492)$, $(m,n,p) = (\frac{1}{4}, \frac{9}{16}, -\frac{4}{9})$ $s_i = (2\times10^{-7}, -2\times10^{-5}, 0.0012, -0.0465, 1.0311)$
24	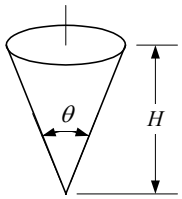 **vertical cone**	$\mathrm{Nu}_L = 0.63(1+0.72\varepsilon)\mathrm{Gr}_L^{1/4}$ $\varepsilon = 2\cot\left(\theta/L\right)\mathrm{Gr}_L^{-1/4}$, $0.2 \le \varepsilon \le 0.8$ laminar or turbulent Oosthuizen and Donaldson[55]	$k_e = 1.6UL\mathrm{Gr}_L^{-1/4}/\left(1+0.72\varepsilon\right)$ $3\times10^7 \le \mathrm{Gr}_L \le 5\times10^8$, $3° \le \theta \le 12°$
25		$\mathrm{Nu}_L = \left[0.735 + \dfrac{0.387\mathrm{Ra}_L^{1/6}}{\left(1+0.671\mathrm{Pr}^{-9/16}\right)^{8/27}}\right]^2$ laminar or turbulent, Churchill[50]	$k_e \rightarrow$ Eq. (57), $\forall\mathrm{Ra}_L$, $L = \frac{4}{5}H$ $a_i = (0.735, 0.387, 0.492)$ $s_i = (4\times10^{-7}, -4\times10^{-5}, 0.0018, -0.0576, 1.0283)$
26		$\mathrm{Nu}_D = 2 + 0.43\mathrm{Ra}_D^{1/4}$ laminar or turbulent, Yuge[56]	$k_e \rightarrow$ Eq. (66), $\forall\mathrm{Ra}_L$, $L = \frac{4}{5}H$ $1 < \mathrm{Gr}_D < 10^5$, $\mathrm{Pr} \sim 1$
27	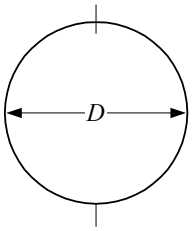 **sphere**	$\mathrm{Nu}_D = 2 + \dfrac{0.589\mathrm{Ra}_D^{1/4}}{\left(1+0.653\mathrm{Pr}^{-9/16}\right)^{4/9}}$ laminar or turbulent, Churchill[50]	$k_e =$ Eq. (36), $\mathrm{Ra}_D \le 10^{11}$, $\mathrm{Pr} > 0.5$, $L = D$ $a_i = (2, 0.589, 0.469)$, $(m,n,p) = (\frac{1}{4}, \frac{9}{16}, -\frac{4}{9})$ $s_i = (2\times10^{-7}, -2\times10^{-5}, 0.0012, -0.0465, 1.0311)$
28		$\mathrm{Nu}_L = \left[1.77 + \dfrac{0.387\mathrm{Ra}_L^{1/6}}{\left(1+0.671\mathrm{Pr}^{-9/16}\right)^{8/27}}\right]^2$ laminar or turbulent, Churchill[50]	$k_e \rightarrow$ Eq. (57), $\forall\mathrm{Ra}_L$, $L = \frac{1}{2}\pi D$ $a_i = (1.77, 0.387, 0.492)$ $s_i = (4\times10^{-10}, -3\times10^{-7}, 6\times10^{-5}, -0.0103, 1.0336)$
29		$\mathrm{Nu}_L = 3.545 + \dfrac{0.685\mathrm{Ra}_L^{1/4}}{\left(1+0.671\mathrm{Pr}^{-9/16}\right)^{4/9}}$ laminar, Yovanovich[51]	$k_e \rightarrow$ Eq. (36), $0 < \mathrm{Ra}_L < 10^8$, $L = \left(\frac{\pi}{3}\right)^{1/2} D$ $a_i = (3.545, 0.685, 0.492)$ $(m,n,p) = (\frac{1}{4}, \frac{9}{16}, -\frac{4}{9})$ $s_i = (2\times10^{-7}, -2\times10^{-5}, 0.0012, -0.0465, 1.0311)$

	Description	Free convection correlation	Effective thermal conductivity
30	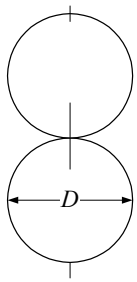 **bi-sphere**	$\mathrm{Nu}_L = 3.475 + \dfrac{0.622\mathrm{Ra}_L^{1/4}}{\left(1+0.671\mathrm{Pr}^{-9/16}\right)^{4/9}}$ laminar, Yovanovich[51]	$k_e \rightarrow$ Eq. (36), $0 < \mathrm{Ra}_L < 10^8$, $L = \left(\frac{2\pi}{3}\right)^{1/2} D$ $a_i = (3.475, 0.622, 0.492)$, $(m,n,p) = (\frac{1}{4}, \frac{9}{16}, -\frac{4}{9})$ $s_i = (2\times10^{-7}, -2\times10^{-5}, 0.0012, -0.0465, 1.0311)$
31	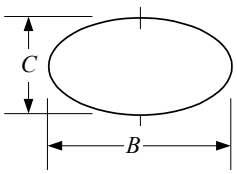 **oblate spheroid**	$\mathrm{Nu}_L = 3.529 + \dfrac{0.651\mathrm{Ra}_L^{1/4}}{\left(1+0.671\mathrm{Pr}^{-9/16}\right)^{4/9}}$ $C/B = 0.5$, laminar, Yovanovich[51]	$k_e \rightarrow$ Eq. (36), $0 < \mathrm{Ra}_L < 10^8$, $L = A_w^{1/2}$ $a_i = (3.529, 0.651, 0.492)$ $(m,n,p) = (\frac{1}{4}, \frac{9}{16}, -\frac{4}{9})$ $s_i = (2\times10^{-7}, -2\times10^{-5}, 0.0012, -0.0465, 1.0311)$
32		$\mathrm{Nu}_L = 3.342 + \dfrac{0.515\mathrm{Ra}_L^{1/4}}{\left(1+0.671\mathrm{Pr}^{-9/16}\right)^{4/9}}$ $C/B = 0.1$, laminar, Yovanovich[51]	$k_e \rightarrow$ Eq. (36), $0 < \mathrm{Ra}_L < 10^8$, $L = A_w^{1/2}$ $a_i = (3.342, 0.515, 0.492)$, $(m,n,p) = (\frac{1}{4}, \frac{9}{16}, -\frac{4}{9})$ $s_i = (2\times10^{-7}, -2\times10^{-5}, 0.0012, -0.0465, 1.0311)$
33	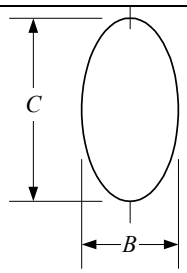 **prolate spheroid**	$\mathrm{Nu}_L = 3.566 + \dfrac{0.678\mathrm{Ra}_L^{1/4}}{\left(1+0.671\mathrm{Pr}^{-9/16}\right)^{4/9}}$ $C/B = 1.93$, laminar, Yovanovich[51]	$k_e \rightarrow$ Eq. (36), $0 < \mathrm{Ra}_L < 10^8$, $L = A_w^{1/2}$ $a_i = (3.566, 0.678, 0.492)$, $(m,n,p) = (\frac{1}{4}, \frac{9}{16}, -\frac{4}{9})$ $s_i = (2\times10^{-7}, -2\times10^{-5}, 0.0012, -0.0465, 1.0311)$
34	**spherelike surface with area A_S and volume $\mathcal{V}$**	$\mathrm{Nu}_L = \left[\dfrac{3\pi\mathcal{V}}{A_S} + \dfrac{0.387\mathrm{Ra}_L^{1/6}}{\left(1+0.671\mathrm{Pr}^{-9/16}\right)^{8/27}}\right]^2$ laminar or turbulent, Churchill[50]	$k_e \rightarrow$ Eq. (36), $\forall \mathrm{Ra}_L$, $L = A_S^{3/2}/(6\mathcal{V})$ $a_i = (3\pi\mathcal{V}/A_S, 0.387, 0.492)$ $s_i = (4\times10^{-10}, -3\times10^{-7}, 6\times10^{-5}, -0.0103, 1.0336)$
35	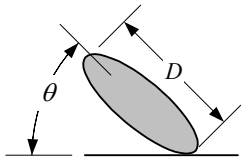 **inclined disk**	$\mathrm{Nu}_L = \left[0.748 + \dfrac{0.387\mathrm{Ra}_L^{1/6}}{\left(1+0.671\mathrm{Pr}^{-9/16}\right)^{8/27}}\right]^2$ laminar or turbulent, Churchill[50]	$k_e \rightarrow$ Eq. (57), $\forall \mathrm{Ra}_L$ $L = \frac{9}{11} D$ $a_i = (0.748, 0.387, 0.492)$ $s_i = (3\times10^{-7}, -3\times10^{-5}, 0.0017, -0.0553, 1.027)$
36	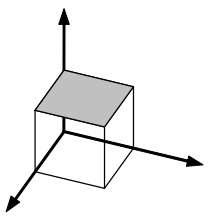 **cube (H^3) with base in plane**	$\mathrm{Nu}_L = 3.388 + \dfrac{0.637\mathrm{Ra}_L^{1/4}}{\left(1+0.671\mathrm{Pr}^{-9/16}\right)^{4/9}}$ laminar, Yovanovich[51]	$k_e \rightarrow$ Eq. (36), $0 < \mathrm{Ra}_L < 10^8$, $L = \sqrt{6}H$ $a_i = (3.388, 0.637, 0.492)$, $(m,n,p) = (\frac{1}{4}, \frac{9}{16}, -\frac{4}{9})$ $s_i = (2\times10^{-7}, -2\times10^{-5}, 0.0012, -0.0465, 1.0311)$

	Description	Free convection correlation	Effective thermal conductivity
37	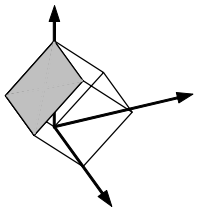 **cube oriented 45° to base plane**	$\mathrm{Nu}_L = 3.388 + \dfrac{0.663\mathrm{Ra}_L^{1/4}}{\left(1+0.671\mathrm{Pr}^{-9/16}\right)^{4/9}}$ laminar, Yovanovich[51]	$k_e \rightarrow$ Eq. (36), $0 < \mathrm{Ra}_L < 10^8$, $L = \sqrt{6}H$ $a_i = (3.388, 0.663, 0.492)$, $(m,n,p) = (\frac{1}{4}, \frac{9}{16}, -\frac{4}{9})$ $s_i = (2\times10^{-7}, -2\times10^{-5}, 0.0012, -0.0465, 1.0311)$
38	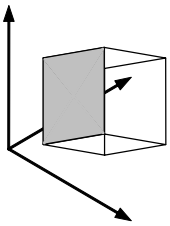 **cube oriented with diagonal $\perp$ to base plane**	$\mathrm{Nu}_L = 3.388 + \dfrac{0.679\mathrm{Ra}_L^{1/4}}{\left(1+0.671\mathrm{Pr}^{-9/16}\right)^{4/9}}$ laminar, Yovanovich[51]	$k_e \rightarrow$ Eq. (36), $0 < \mathrm{Ra}_L < 10^8$, $L = \sqrt{6}H$ $a_i = (3.388, 0.679, 0.492)$, $(m,n,p) = (\frac{1}{4}, \frac{9}{16}, -\frac{4}{9})$ $s_i = (2\times10^{-7}, -2\times10^{-5}, 0.0012, -0.0465, 1.0311)$

In the less probable case of $\Delta \geq 0$, an ordinary root is precipitated. One gets

$$k_e = \tfrac{1}{6}b_2 + \tfrac{2}{3}b_0^2 b_2^{-1} - \tfrac{1}{3}b_0 ;$$

$$b_2 \equiv \left(108b_1 - 8b_0^3 + 12\sqrt{81b_1^2 - 12b_0^3 b_1}\right)^{1/3} \qquad (12)$$

The trigonometric root may be safely used in most chip cooling applications where the characteristic length L is on the order of $\mathrm{Gr}_L \mu C_P / U$ or larger. Equation (12) should be defaulted to under the rare circumstances in which fails.

For turbulent flows, Eq. (8) yields a fourth order polynomial. The meaningful root that ensues can be written as

$$k_e = \left(\sqrt{2 + 2(1+c_1)^{-1/2} - c_1} - 1 - \sqrt{1-c_1}\right)c_0^{-1} \qquad (13)$$

where

$$c_0 \equiv (a_1/a_0)^4 \mathrm{Gr}_L \mu C_P, \; c_1 \equiv 2\left(\tfrac{2}{3}c_2 c_3\right)^{1/3} \times\left[\left(\tfrac{2}{3}\right)^{1/3} - 8c_2^{1/3}c_3^{-2/3}\right]c_0^{-2} \qquad (14)$$

$$c_2 \equiv (UL/a_0)^4, \; c_3 \equiv \sqrt{81c_0^4 + 768c_2} - 9c_0^2$$

V. Approximate k_e for Laminar Free Convection

The difficulty arises when considering the familiar expression (e.g., Churchill and Chu[40])

$$\mathrm{Nu}_L = UL/k_e = a_0 + a_1 \mathrm{Ra}_L^m \left[1 + \left(a_2/\mathrm{Pr}\right)^n\right]^p \qquad (15)$$

which can be obtained by setting $p = mr$ in Eq. (5). This relation applies to a number of important shapes whose characteristic constants are furnished in Table 1. In short, the difficulty stems from k_e being simultaneously present in the Nusselt, Rayleigh and Prandtl numbers. This can be seen by rearranging (15) into

$$UL/k_e = a_0 + a_1\left(A_0/k_e\right)^m \left\{1 + \left[a_2 k_e/(\mu C_P)\right]^n\right\}^p ;$$

$$A_0 \equiv \mu C_p \mathrm{Gr}_L \qquad (16)$$

The power-law embedment of k_e in the universal Prandtl number function given by (4) eliminates the possibility of obtaining an exact expression for k_e. An asymptotic approximation of the form $k_e \approx k_0 + k_1$ will have to be settled for. To proceed, the Prandtl number function has to be expanded first. Letting $\kappa = a_2/\mu C_p$, it follows that two cases must be considered separately depending on the size of U, and therefore, k_e.

A. Type-I: Laminar Regime, Small U Case

For small κk_e, one can expand (4) straightforwardly viz.

$$\left[1 + \left(\kappa k_e\right)^n\right]^p = 1 + p\left(\kappa k_e\right)^n + \tfrac{p(p-1)}{2!}\left(\kappa k_e\right)^{2n} + \tfrac{p(p-1)(p-2)}{3!}\left(\kappa k_e\right)^{3n} + \tfrac{p(p-1)(p-2)(p-3)}{4!}\left(\kappa k_e\right)^{4n} + \ldots \qquad (17)$$

By substituting Eq. (17) into Eq. (16), one gathers the multi-order polynomial

$$UL = \underset{1}{a_0}k_e + \underset{2}{B_0}k_e^{1-m} + \underset{(-)}{C_0}k_e^{1-m+n} + \underset{3}{D_0}k_e^{1-m+2n} + \underset{(-)}{E_0}k_e^{1-m+3n} + \underset{4}{F_0}k_e^{1-m+4n} \qquad (18)$$

where,

$$\begin{cases} B_0 \equiv a_1 A_0^m, \quad C_0 \equiv pB_0\kappa^n \\ D_0 \equiv \frac{p(p-1)}{2!} B_0\kappa^{2n}, \quad E_0 \equiv \frac{p(p-1)(p-2)}{3!} B_0\kappa^{3n} \\ F_0 \equiv \frac{p(p-1)(p-2)(p-3)}{4!} B_0\kappa^{4n} \end{cases} \tag{19}$$

It should be noted that, in our search for the most influential term in Eq. (18), quantities that are negative have been discounted as they lead to unphysical thermal conductivities. By considering each of the four enumerated terms as leading-order candidates, the zeroth-order expression for k_e is narrowed down to

$$k_e = \left\{ UL/a_0, (UL/B_0)^{1/(1-m)}, (UL/D_0)^{1/(1-m+2n)}, (UL/F_0)^{1/(1-m+4n)} \right\} \tag{20}$$

These terms are plotted in Figure 1 alongside the numerical solution. This is carried out for three different geometric shapes to ensure portability. From the plot, it is clear that Term 2 has the most influence since it closely approximates the numerical solution. The parameters used in this comparison correspond to a commercial heat sink modeled by Narasimhan and Majdalani.[28] It is characterized by $L = 0.0762\,\mathrm{m}$, $A_b = 0.00314\,\mathrm{m}^2$, $\rho = 1.1\,\mathrm{kg m^{-3}}$, $T_b = 293.15\,\mathrm{K}$, $\mu = 1.95\times10^{-5}\,\mathrm{kg m s^{-1}}$, and $C_p = 1,007\,\mathrm{J kg^{-1} K^{-1}}$. By trying other cases, the dominant position of Term 2 is found to be rather independent of this particular choice of operating parameters. Having identified $k_0 = (UL/B_0)^{1/(1-m)}$, the next step is to put

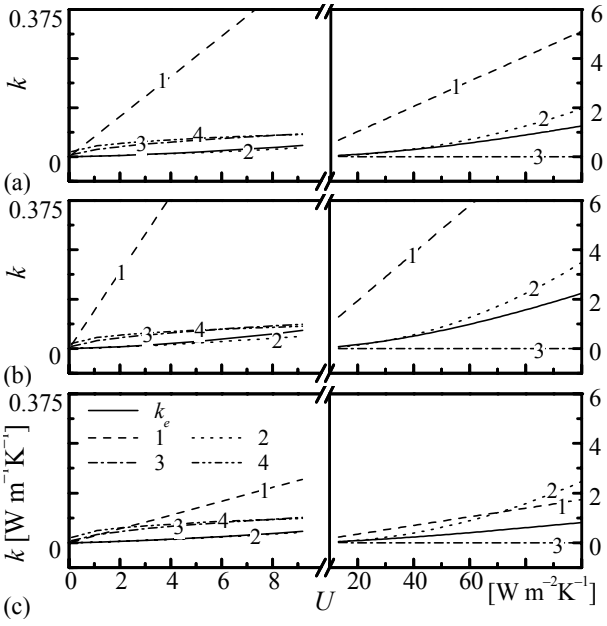

Fig. 1 Relative size of leading terms arising in the expansion of the universal Nusselt number correlation for free convection laminar flow over (a) vertical plates, (b) cylinders, and (c) spheres. Note that while Term 1 dominates for small *U*, both Terms 1 and 2 are simultaneously needed to evaluate the leading order term of the large–*U* approximation.

$$k_e^1 = \left(UL/B_0\right)^{1/(1-m)} + k_1 \tag{21}$$

where the superscript is used to denote a type-I solution. To solve for the first-order correction k_1, the notion of successive approximations is used. Accordingly, Eq. (21) is substituted back into Term 2 of Eq. (18) while only the leading-order part k_0 is used in the remaining terms. This permits extracting k_1 from

$$a_0k_0^2 + (1-m)ULk_1 + C_1k_0^{2-m+n} + D_0k_0^{2-m+2n} + E_0k_0^{2-m+3n} + F_0k_0^{2-m+4n} = 0 \tag{22}$$

thus yielding

$$k_1 = -\left[UL(1-m)\right]^{-1}\left(a_0k_0^2 + C_0k_0^{2-m+n} + D_0k_0^{2-m+2n} + E_0k_0^{2-m+3n} + F_0k_0^{2-m+4n}\right). \tag{23}$$

Equation (21) is valid for all L and B_0 as long as $0 \le k_e^1 \le k_{//}$ where $k_{//}$ is a cut-off value that varies on average between 0.01 and 0.13 $\mathrm{W m^{-1} K^{-1}}$. This physical limitation is due to the divergence of the Taylor series at larger values of U.

B. Type-II: Laminar Regime, Large U Case

Recalling that the thermal conductivity of the artificial block of fluid is commensurate with the overall heat transfer coefficient of the actual heat sink, the series expansion in Eq. (17) can become divergent as U is increased. When κk_e is no longer small, one needs to re-expand Eq. (17) in the reciprocal of κk_e. One obtains

$$\left(\kappa k_e\right)^{np}\left[1+1/\left(\kappa k_e\right)^n\right]^p = \left(\kappa k_e\right)^{np}\left[1 + p\left(\kappa k_e\right)^{-n} + \frac{p(p-1)}{2!}\left(\kappa k_e\right)^{-2n} + \frac{p(p-1)(p-2)}{3!}\left(\kappa k_e\right)^{-3n} + \ldots\right] \tag{24}$$

When Eq. (24) is substituted back into Eq. (16), a number of terms arise. Some are so small that they can be ignored. The remaining terms are found to be

$$UL = \underset{1}{a_0k_e} + \underset{2}{B_1k_e^{1+np-m}} + \underset{(-)}{C_1k_e^{1-n+np-m}} + \underset{3}{D_1k_e^{1-2n+np-m}} + \underset{(-)}{E_1k_e^{1-3n+np-m}}; \tag{25}$$

$$\begin{cases} B_1 \equiv B_0\kappa^{np}, \quad C_1 \equiv B_0p\kappa^{np-n} \\ D_1 \equiv \frac{p(p-1)}{2!} B_0\kappa^{np-2n}, \quad E_1 \equiv \frac{p(p-1)(p-2)}{3!} B_0\kappa^{np-3n} \end{cases} \tag{26}$$

By dismissing negative terms that cannot possibly dominate the solution, three terms are identified in (25) as possible leading-order candidates. These are

$$k_e = \left\{ UL/a_0, (UL/B_1)^{1/(1+np-m)}, \right.$$
$$\left. (UL/D_1)^{1/(1-2n+np-m)} \right\} \quad (27)$$

By comparing these approximations to the exact solution in Figure 1, one realizes that no single term dominates by itself. Rather, one finds that the leading-order behavior is prescribed by the balance of Terms 1 and 2. Assuming a type-II expansion of the form $k_e^{\mathrm{II}} \approx K_0 + K_1$, the corresponding solution must be produced from

$$-UL + a_0 K_0 + B_1 K_0^{1+np-m} = 0 \quad (28)$$

Fortuitously, all cases presented in this paper are characterized by a single exponent, $1 + np - m = 1/2$. This simplifying power leads to a quadratic equation. Based on the meaningful quadratic root, the two-term expansion for k_e^{II} becomes

$$k_e^{\mathrm{II}} = \left[UL + \tfrac{1}{2} B_1 \left(B_1 - \sqrt{B_1^2 + 4a_0 UL} \right) / a_0 \right] / a_0 + K_1 \quad (29)$$

Using successive approximations, Eq. (29) is now substituted into Terms 1 and 2 of Eq. (25). However, only K_0 is substituted in all other occurrences of k_e^{II}. Once completed, K_1 is found to be

$$K_1 = 16 k_0 \left(E_1 + D_1 K_0^{9/16} + C_1 K_0^{9/8} \right)$$
$$/ \left(19E_1 + 10 D_1 K_0^{9/16} + C_1 K_0^{9/8} - 8 B_1 K_0^{27/16} - 16 a_0 K_0^{35/16} \right) \quad (30)$$

For the more general case of an arbitrary exponent in Eq. (28), the correction K_1 takes the form

$$K_1 = K_0 \left(E_1 K_0^{2+2np-2m-3n} + D_1 K_0^{2+2np-2m-4n} \right.$$
$$+ C_1 K_0^{2+2np-2m-5n} + B_1 K_0^{4+4np-4m-6n} \Big)$$
$$/ \left(E_1 (1 + np - m - 3n) K_0^{2+2np-2m-3n} \right.$$
$$+ D_1 (1 + np - m - 2n) K_0^{2+2np-2m-4n}$$
$$+ B_1 C_1 (1 - n + np - m) K_0^{2+2np-2m-5n}$$
$$\left. - a_0 K_0^{5+4np-4m-6n} - B_1 K_0^{4+4np-4m-6n} \right) \quad (31)$$

Equation (29) is valid for all L and B_1 as long as $k_e^{\mathrm{II}} > k_{//}$. Again, the range of applicability is limited by the divergence of the Taylor series expansion involved in the solution.

C. Cut-off Value $k_{//}$

The cut-off value that delimits the small and large k_e solutions can be determined by carefully examining the convergence criteria for the two cases at hand. Based on Eq. (17), the requirement for the type-I expansion can be seen to be $|p(\kappa k_e)^n| < 1$. The small series expansion will thus diverge whenever

$$k_e < k_e^+ ; \; k_e^+ \equiv |p^{-1/n} \kappa^{-1}| \quad (32)$$

In like manner, the large series expansion in Eq. (24) will diverge with $|p(\kappa k_e)^{-n}| < 1$ or

$$k_e > k_e^- ; \; k_e^- \equiv |p^{1/n} \kappa^{-1}| \quad (33)$$

The presence of two asymptotic bounds motivates the search for a cut-off $k_{//} \in [k_e^-, k_e^+]$ that can be taken as the simultaneous upper and lower caps for the type-I and type-II approximations. By setting

$$k_{//} = x k_e^- + (1 - x) k_e^+ ; \; x \in [0,1] \quad (34)$$

x is then chosen in a manner to minimize the maximum asymptotic error in both k_e^{I} and k_e^{II}. After some effort, the optimal value is computed and correlated using a polynomial of the form

$$x = s_0 + s_1 \bar{k} + s_2 \bar{k}^2 + s_3 \bar{k}^3 + s_4 \bar{k}^4 ; \; \bar{k} = 2UL/(k_e^- + k_e^+) \quad (35)$$

where the $s_i = (s_0, s_1, s_2, s_3)$ coefficients are provided in Table 1. These constants are determined using a parametric study involving 2,000 runs per geometric shape and a correlation coefficient exceeding 0.998. Using Eq. (35), the maximum asymptotic error at the delineation point where both approximations are optimally patched is contained within 2% if k_e is at least 5% away from $k_{//}$. In practice, once the cut-off $k_{//}$ is calculated for a given heat sink application, one may safely use the appropriate correlation depending on the operating range viz.

$$k_e = \begin{cases} k_e^{\mathrm{I}}; & 0 < k_e \le k_{//} \\ k_e^{\mathrm{II}}; & k_e > k_{//} \end{cases} \quad \text{(laminar regime)} \quad (36)$$

where both approximations are equivalent at the cut-off point. The degree of precision associated with Eqs. (21) and (29) is illustrated in Figure 2 where analytical and numerical predictions for k_e are compared over a wide range of U and three basic configuration shapes.

VI. Approximate k_e for Laminar and Turbulent Free Convection

For a broader correlation that remains applicable under turbulent conditions, Churchill and Chu[40] have introduced an expression for flow over a flat plate that has also been adopted in diverse physical settings. Theirs can be generically written as

$$\mathrm{Nu}_L = UL/k_e = \left\{ a_0 + a_1 \mathrm{Ra}^{m/2} \left[1 + (a_2/\mathrm{Pr})^n \right]^{p/2} \right\}^2 \quad (37)$$

Clearly, Eq. (37) can be restored from Eq. (6) when $q=2$. To make headway, one uses a quadratic expansion to expose individual exponents via

$$UL/k_e = a_0^2 + 2a_0a_1\,\mathrm{Ra}^{m/2}\left[1+(a_2/\mathrm{Pr})^n\right]^{p/2} + \left\{a_1\,\mathrm{Ra}^{m/2}\left[1+(a_2/\mathrm{Pr})^n\right]^{p/2}\right\}^2 \quad (38)$$

Subsequently, one may set $A_2 \equiv (g\beta\Delta TL^3\rho^2C_p/\mu)^{m/2}$ and rearrange Eq. (38) into

$$UL = a_0^2k_e + 2a_0a_1k_e^{1-m/2}A_2\left\{1+\left[a_2k_e/(\mu C_P)\right]^n\right\}^{p/2} + a_1^2k_e^{1-m}A_2^2\left\{1+\left[a_2k_e/(\mu C_P)\right]^n\right\}^p \quad (39)$$

From Eq. (39) a solution for k_e must be carefully obtained based on the size of U. Following the lines described previously, two asymptotic approximations can be constructed for small and large U.

A. Type-I: Dual Regime, Small U Case

To ensure convergence to the desired solution $k_e \approx k_0 + k_1$, we first put $w=[a_2k_e/(\mu C_p)]^n$ into Eq. (39). This yields

$$UL = a_0^2k_e + 2a_0a_1A_2k_e^{1-m/2}T_1 + a_1^2A_2^2k_e^{1-m}T_2 \quad (40)$$

where

$$\begin{cases} T_1 = 1-\frac{1}{2}pw+\frac{1}{8}p(p-2)w^2+\ldots \\ T_2 = 1-pw+\frac{1}{2}p(p-1)w^2+\ldots \end{cases}, \quad (41)$$

At this point the powers of k_e can be exposed by inserting Eq. (41) into Eq. (40). One gets

$$UL = a_0^2k_e + 2a_0a_1A_2\left[k_e^{1-m/2} - \tfrac{1}{2}puk_e^{1-m/2+n} + \tfrac{1}{8}p(p-2)u^2k_e^{1-m/2+2n}\right] + a_1^2A_2^2 \times\left[k_e^{1-m} - puk_e^{1-m+n} + \tfrac{1}{2}p(p-1)u^2k_e^{1-m+2n}\right];$$

$$u \equiv \left(a_2/\mu C_P\right)^n \quad (42)$$

For the specific constants (m,n,p) listed in Table 1, the leading order term for this solution can be obtained following Brucker and Majdalani.[57] The result is

$$k_0 = a_1^{-2/(1-m)}A_2^{-2/(1-m)}(UL)^{1/(1-m)} \quad (43)$$

which, for $m=1/3$, yields

$$k_0 = a_1^{-3}A_2^{-3}(UL)^{3/2} \quad (44)$$

The final solution can be obtained from

$$k_e^{\mathrm{I}} = a_1^{-3}A_2^{-3}(UL)^{3/2} + k_1 + k_n \quad (45)$$

where

$$k_1 = -\tfrac{3}{2}\Big[a_0^2k_0^2 + 2a_0a_1A_2\left(k_0^{11/6} - \tfrac{8}{27}uk_0^{115/48} + \tfrac{140}{729}u^2k_0^{71/24}\right) + a_1^2A^2u\left(\tfrac{344}{729}uk_0^{67/24} - \tfrac{16}{27}k_0^{107/48}\right)\Big]/(UL) \quad (46)$$

The higher-order corrections at $n=2,3,\ldots$ can be recovered from the recurrence relation

$$k_n = -\tfrac{3}{2}k_0k_{n-1}\Big[a_0^2 + a_0a_1A_2\left(\tfrac{5}{3}k_0^{-1/6} - \tfrac{67}{81}uk_0^{19/48} + \tfrac{1645}{2187}u^2k_0^{23/24}\right) + a_1^2A_2^2u\left(\tfrac{1849}{2187}uk_0^{19/24} - \tfrac{59}{81}k_0^{11/48}\right)\Big]/(UL) \quad (47)$$

In Brucker and Majdalani,[57] a two-term approximation for Eq. (45) based on Eq. (44) and Eq. (46) was found to be sufficiently adequate for problems of practical interest. This was realized by comparing results from the compact model with experimental and detailed numerical simulations. Here too, Eq. (45) is valid for all L and A_2 so long as $0 < k_e^{\mathrm{I}} \le k_{//}$.

B. Type-II: Dual Regime, Large U Case

In this case, the universal Prandtl number function must be expanded in the reciprocal of κk_e. This turns Eq. (39) into

$$UL = a_0^2k_e + 2a_0a_1A_2u^{-p/2}k_e^{1-m/2+np/2} + a_1^2A_2^2u^pk_e^{1-m+np} - pa_1^2A_2^2u^{-p-1}k_e^{1-m-np-n} \quad (48)$$

As usual, terms that are not shown have an insignificant contribution. In seeking the leading-order solution, we include all except the last term in Eq. (48). The problem becomes that of solving

$$-c_1 + c_2k_e^{1-m/2+np/2} + c_3k_e^{1-m+np} + c_4k_e = 0 \quad (49)$$

where

$$\begin{cases} c_1 \equiv UL, \quad c_2 \equiv a_1^2A_2^2u^p \\ c_3 \equiv 2a_0a_1A_2u^{p/2}, \quad c_4 \equiv a_0^2 \end{cases} \quad (50)$$

In the specific cases listed in Table 1, Eq. (49) leads to a cubic, namely

$$-c_1 + c_2k_e^{1/3} + c_3k_e^{2/3} + c_4k_e = 0 \quad (51)$$

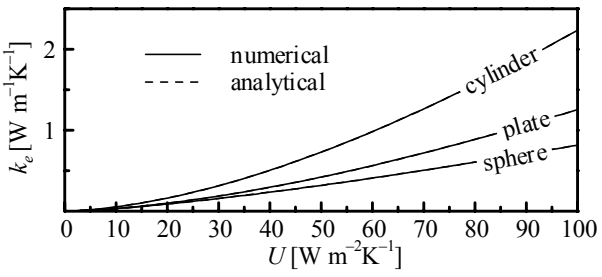

Fig. 2 Numerical verification of the analytical solutions obtained for three geometric shapes and typical operating parameters.

Using $k_e^{\mathrm{II}} \approx K_0 + K_1$ as before, the meaningful root in Eq. (51) can be exacted from

$$K_0 = \left(c_1 - c_3 p_1^2 - c_2 p_2\right)/c_4 \tag{52}$$

where

$$\begin{cases} p_0 \equiv (36c_2c_3c_4 + 108c_1c_4^2 - 8c_3^3 + p_2)^{1/3} \\ p_1 \equiv \frac{1}{6}\, p_0/c_4 - \frac{2}{3}(3c_2c_4 - c_3^2)/(c_4 p_0) - \frac{1}{3}(c_3/c_4) \\ p_2 \equiv 12\sqrt{3}c_4\left(27c_1^2c_4 - c_2^2c_3^2 - 4c_1c_3^3 + 4c_2^3c_4 + 18c_1c_2c_3c_4\right)^{1/2} \end{cases} \tag{53}$$

In order to account for the small correction associated with the fourth term in Eq. (48), one can substitute the result back into the expanded Churchill and Chu correlation and solve for the linear correction term,

$$K_1 = -\tfrac{16}{9} a_1^2 A_2^2 K_0^{-11/48} u^{-43/27} \Big/ \left(3a_0^{\,2} + 4a_0 a_1 A_2 K_0^{-1/3} u^{-8/27} + a_1^2 A_2^2 K_0^{-2/3} u^{-16/27}\right) \tag{54}$$

Equations (52) and (54) are valid for all L and c_i so long as $k_e^{\mathrm{II}} > k_{//}$.

C. Cut-off Value $k_{//}$

The cut-off value in the dual regime can be obtained following the lines described in Section V.C. The difference is that the current solution depends on two Taylor series for each approximation, as opposed to only one. This can be seen by realizing that both expansions in Eq. (41) will diverge for small U unless $|\tfrac{1}{2} puk_e^n| < 1$ and $|puk_e^n| < 1$. Both criteria are fulfilled when

$$k_e < k_e^+;\ k_e^+ \equiv |(pu)^{-1/n}| \tag{55}$$

In like manner, the large U expansion diverges unless $|\tfrac{1}{2} pu^{-1}k_e^{-n}| < 1$ and $|pu^{-1}k_e^{-n}| < 1$. This is true when

$$k_e > k_e^-;\ k_e^- \equiv |(p/u)^{1/n}| \tag{56}$$

Once again, the procedure summarized in Eqs. (34)–(35) can be used to determine the optimal $k_{//}$. After 2000 runs per geometric shape, the coefficients of the best fit polynomial are determined with a correlation coefficient exceeding 0.998. In comparison to the numerical solution, the asymptotic result based on patching both solutions at $k_{//}$ deviates by no more than 2% provided that one is at least 5% away from the delineation point. The final solution is expressible by the piecewise form given by Eq. (36), namely,

$$k_e = \begin{cases} k_e^{\mathrm{I}}; & 0 < k_e \le k_{//} \\ k_e^{\mathrm{II}}; & k_e > k_{//} \end{cases} \text{ (laminar and turbulent)} \tag{57}$$

VII. General Forced Convection

Numerous empirical correlations are available for predicting forced convection heat transfer from bodies of various shapes. Generally, these correlations can be abbreviated by using generic forms that depend on the flow regime. In particular, one may write

$$\mathrm{Nu}_L = \begin{cases} C_l\, \mathrm{Re}_L^m\, \mathrm{Pr}^n, \text{ laminar} \\ C_t\, \mathrm{Re}_L^p\, \mathrm{Pr}^q, \text{ turbulent} \end{cases} \tag{58}$$

$$\text{for which } \mathrm{Nu}_x = \begin{cases} mC_l\, \mathrm{Re}_x^m\, \mathrm{Pr}^n, \text{ laminar} \\ pC_t\, \mathrm{Re}_x^p\, \mathrm{Pr}^q, \text{ turbulent} \end{cases} \tag{59}$$

Based on these two relations for average and local Nusselt numbers, one can integrate for the combined laminar and turbulent flow correlation if the critical Reynolds number $\mathrm{Re}_{\mathrm{cr}}$ is known for the case at hand. One finds

$$\mathrm{Nu}_L = [C_t\, \mathrm{Re}_L^p - (C_t\, \mathrm{Re}_{\mathrm{cr}}^{p-m} - C_l)\, \mathrm{Re}_{\mathrm{cr}}^m]\, \mathrm{Pr}^q;\ n = q. \tag{60}$$

For flow over an isothermal plate, one may use $C_l = 0.664$, $C_t = 0.037$, $m = 1/2$, $p = 4/5$, $n = q = 1/3$, and $\mathrm{Re}_{\mathrm{cr}} = 5 \times 10^5$ to verify that $\mathrm{Nu}_L = (0.037\, \mathrm{Re}_L^{4/5} - 871.3)\, \mathrm{Pr}^{1/3}$.[1] When the base plate is subjected to a sufficiently uniform heat flux, only leading coefficients in Eq. (59) need to be modified. By setting $C_l = 0.906$ and $C_t = 0.0385$, the corresponding correlation becomes $\mathrm{Nu}_L = (0.0385\, \mathrm{Re}_L^{4/5} - 754.6)\, \mathrm{Pr}^{1/3}$. It should be noted that in most compact models, an isothermal surface temperature is assumed even in the presence of a uniform heat flux. This is justified by virtue of the small surface area and large conductivity of the base plate.

Ordinarily, regardless of the correlation used for forced convection, determination of the effective thermal conductivity is straightforward. This can be accomplished by setting $\mathrm{Nu}_L = UL/k_e$ in Eqs. (59)–(60) and solving for k_e. The result is

$$k_e = \begin{cases} \mathrm{Re}_L^m\, \mu Cp[UL/(C_l\, \mathrm{Re}_L^m\, \mu Cp)]^{1/(1-n)}, & \text{laminar} \\ \mathrm{Re}_L^p\, \mu Cp[UL/(C_t\, \mathrm{Re}_L^p\, \mu Cp)]^{1/(1-q)}, & \text{turbulent} \\ \left\{ \begin{array}{l} UL \\ /[C_t\, \mathrm{Re}_L^p - (C_t\, \mathrm{Re}_{\mathrm{cr}}^{p-m} - C_l)\, \mathrm{Re}_{\mathrm{cr}}^m (\mu Cp)^q] \end{array} \right\}^{1/(1-q)} & \\ \quad n = q, \text{ combined laminar and turbulent} & \end{cases} \tag{61}$$

Equation (61) is instrumental in determining k_e for several shapes used in forced convection studies. These are summarized in Table 2 and include empirical constants due to Jacob.[58] The latter pertain to planar cross-sections whose correlations collapse into the simple expression

$$\mathrm{Nu}_L = C\, \mathrm{Re}_L^m\, \mathrm{Pr}^{1/3} \text{ or } k_e = \left\{UL/\left[C\, \mathrm{Re}_L^m \left(\mu C_P\right)^{1/3}\right]\right\}^{3/2} \tag{62}$$

It may be instructive to note that, for flow over a flat plate, the special equation used in a recent study by Narasimhan and Majdalani[27,28] or Narasimhan, Bar-Cohen and Nair[37] can be restored from Eq. (61). In these studies, results based on Eq. (61) were shown to fall within ±7% of both computational and experimental measurements.

VIII. Approximate k_e for Laminar and Turbulent Forced Convection Across a Sphere

Some correlations exist for which a standalone diffusive constant is added to the term containing the Prandtl number. An illustrative case arises in the context of a laminar or turbulent flow across a sphere of diameter D. This form of the equation applies to the natural convection correlation proposed by Yuge[56] for laminar heat transfer from a sphere. The pertinent Nusselt number relation has been developed by Whitaker[59] over the range $3.5 \le \mathrm{Re}_D \le 7.6\times10^4$ and $0.7 \le \mathrm{Pr} \le 380$. It exhibits the form

$$\mathrm{Nu}_D = C_0 + C_1 \mathrm{Pr}^n ;\ n \equiv 2/5,\ C_0 \equiv 2,$$

$$C_1 \equiv (0.4\,\mathrm{Re}_D^{1/2} + 0.06\,\mathrm{Re}_D^{2/3})(\mu/\mu_s)^{1/4} \qquad (63)$$

where both C_0 and C_1 are independent of k_e. Equation (63) can be rearranged into

$$k_e + Ak_e^m - B = 0 ;\ m \equiv 1-n,\ A \equiv (\mu C_p)^n (C_1/C_0),$$

$$B \equiv UD/C_0 \qquad (64)$$

then solved asymptotically. Since all physical problems exhibit $0 < n < 1$, a reasonably accurate two-term expansion can be obtained from

$$\left\{ Ak_0^m - B = 0,\ k_0 \ \text{small},\ \ K_0 - B = 0,\ K_0 \ \text{large} \right\} \qquad (65)$$

or

$$k_e = \begin{cases} \dfrac{m}{1/B + m(A/B)^{1/m}}, & k_e \le k_{//} \\ B\left[1 - 1/(m + B^{1-m}/A)\right], & k_e > k_{//} \end{cases} \qquad (66)$$

where the maximum error remains bounded within ±9.1% for $n \le 0.4$. The delimiting value for the small range is $k_{//} = (0.08 + 0.727m - 0.314m^2)A$.

For $0 < n \le 0.4$, the error remains bounded within ±2.5%; furthermore, the range for $k_{//}$ reduces to $0.40 \le k_{//}/A < 0.50$.

IX. Other Correlations

The analytical expressions obtained in the preceding sections enable us to provide direct estimates for k_e in diverse physical settings. This is due to the foregoing generalizations being applicable to a considerable number of flow regimes and geometric configurations. Exact or approximate solutions for k_e can now be instantly determined for a number of geometric shapes starting with the widely used flat plate model. Based on their fundamental correlations found in the literature, these different cases have been compiled and included in Tables 1 and 2 for free and forced convection, respectively. It should be noted that some common shapes exhibit multiple correlations depending on the choice of coolant and characteristic ranges. When such is the case, multiple solutions are provided as well. Of particular use to compact models are flows along or across arbitrarily inclined flat plates, disks, and squares. Circular cross-sections become suitable, for instance, when tube-mounted heat sinks are being considered. These can be helpful in modeling a series of heat sinks mounted along a heat pipe. When a three-dimensional component is being cooled from all sides, three-dimensional objects such as tetrahedrons and spheroids may be resorted to. Although some models may not be immediately essential to ongoing industrial designs, they can still hold value in the rapidly developing research into advanced cooling technologies. This is especially true in view of current realizations for the need to explore 'shelf technologies' that provide thermal analysts with the valuable and much desired lead-time for future implementation. Since the compact k_e value associated with longitudinal flow over a flat plate has been previously validated under free and forced convection conditions, it is hoped that the results derived for other configurations will be further explored in future tests.

Table 2 Effective thermal conductivity of common geometric shapes under forced convection

	Description	Forced convection correlation	Effective thermal conductivity
1	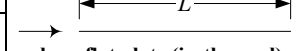 along flat plate (isothermal)	$\mathrm{Nu}_L = 0.664\mathrm{Re}_L^{1/2}\mathrm{Pr}^{1/3}$ laminar[60]	$k_e = \left\{UL/[0.664\,\mathrm{Re}_L^{1/2}(\mu C_P)^{1/3}]\right\}^{3/2}$ $\mathrm{Re}_L \le 5\times10^5,\ \mathrm{Pr} \ge 0.6$
2		$\mathrm{Nu}_L = 0.037(\mathrm{Re}_L^{4/5} - 871)\mathrm{Pr}^{1/3}$ laminar or turbulent[60]	$k_e = \left\{UL/[0.037(\mathrm{Re}_L^{4/5} - 871)(\mu C_P)^{1/3}]\right\}^{3/2}$ $5\times10^5 \le \mathrm{Re}_L \le 10^8,\ 0.6 \le \mathrm{Pr} \le 60$

	Description	Forced convection correlation	Effective thermal conductivity
3		$\mathrm{Nu}_L = 0.906\mathrm{Re}_L^{1/2}\mathrm{Pr}^{1/3}$ ($\dot{Q} = \text{const}$) laminar[1]	$k_e = \left\{UL/[0.906\,\mathrm{Re}_L^{1/2}(\mu C_P)^{1/3}]\right\}^{3/2}$ $\mathrm{Re}_L \le 5\times10^5$, $\mathrm{Pr} \ge 0.6$
4		$\mathrm{Nu}_L = (0.0385\,\mathrm{Re}_L^{4/5} - 755)\,\mathrm{Pr}^{1/3}$ ($\dot{Q} = \text{const}$) laminar or turbulent[1]	$k_e = \left\{UL/[0.0385(\mathrm{Re}_L^{4/5} - 755)(\mu C_P)^{1/3}]\right\}^{3/2}$ $5\times10^5 \le \mathrm{Re}_L \le 10^8$, $0.6 \le \mathrm{Pr} \le 60$
5	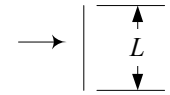 **across vertical flat plate**	$\mathrm{Nu}_L = 0.2\mathrm{Re}_L^{2/3}$ laminar or turbulent, Sogin[61]	$k_e = 5UL\,\mathrm{Re}_L^{-2/3}$ $1 \le \mathrm{Re}_L \le 4\times10^5$, $\mathrm{Pr} = 0.7$
6	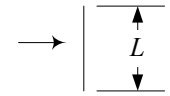 **across square plate**	$\mathrm{Nu}_L = 0.93\mathrm{Re}_L^{1/2}\,\mathrm{Pr}^{1/3}$ laminar or turbulent, Tien and Sparrow[62]	$k_e = \{UL/[0.93\,\mathrm{Re}_L^{1/2}(\mu C_P)^{1/3}]\}^{3/2}$ $2\times10^4 \le \mathrm{Re}_L \le 10^5$, air
7	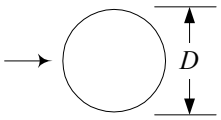 **across sphere**	$\mathrm{Nu}_D = 2 + (0.4\,\mathrm{Re}_D^{1/2} + 0.06\,\mathrm{Re}_D^{2/3})\,\mathrm{Pr}^{0.4}$ $\times(\mu/\mu_s)^{1/4}$ laminar or turbulent, Whitaker[59]	$k_e \rightarrow$ Eq. (66) $3.5 \le \mathrm{Re}_D \le 7.6\times10^4$, $0.7 \le \mathrm{Pr} \le 380$
8	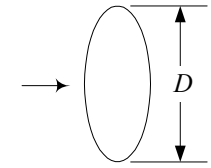 **across disk**	$\mathrm{Nu}_D = 1.05\,\mathrm{Re}_D^{1/2}\,\mathrm{Pr}^{0.36}$ turbulent, Sparrow and Geiger[63]	$k_e = \{UD/[1.05\,\mathrm{Re}_D^{1/2}(\mu C_P)]\}^{1.563}$ $5\times10^3 \le \mathrm{Re}_D \le 5\times10^4$, $0.7 \le \mathrm{Pr} \le 380$
9	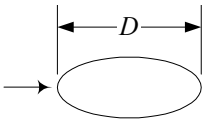 **along disk**	$\mathrm{Nu}_D = 0.591\mathrm{Re}_D^{0.564}\,\mathrm{Pr}^{1/3}$ laminar or turbulent, Wedekind[64]	$k_e = \{UD/[0.59\,\mathrm{Re}_D^{0.564}(\mu C_P)]\}^{3/2}$ $9\times10^2 \le \mathrm{Re}_D \le 3\times10^4$, $0.7 \le \mathrm{Pr} \le 380$

	Geometry[58]	*C*	*n*	Range
10	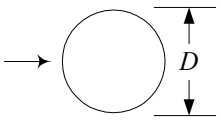	0.989	0.330	$0.4 < \mathrm{Re}_D < 4$
11		0.911	0.385	$4 < \mathrm{Re}_D < 40$
12		0.683	0.466	$40 < \mathrm{Re}_D < 4\times10^4$
13		0.193	0.618	$4\times10^4 < \mathrm{Re}_D < 4\times10^5$
14		0.0266	0.805	$4\times10^5 < \mathrm{Re}_D < 4\times10^6$
15	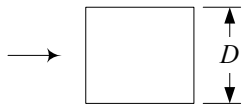	0.104	0.675	$5\times10^4 < \mathrm{Re}_D < 1\times10^6$
16		0.180	0.699	$2.5\times10^4 < \mathrm{Re}_D < 8\times10^4$
17	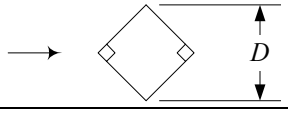	0.251	0.588	$5\times10^4 < \mathrm{Re}_D < 1\times10^6$
18		0.293	0.624	$2.5\times10^4 < \mathrm{Re}_D < 7.5\times10^4$
19	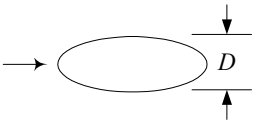	0.252	0.612	$2.5\times10^4 < \mathrm{Re}_D < 1.5\times10^5$

20	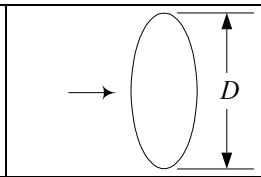	0.096	0.804	$3\times10^4 < \mathrm{Re}_D < 1.5\times10^5$
21	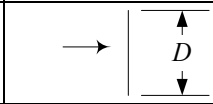	0.232	0.731	$4\times10^4 < \mathrm{Re}_D < 1.5\times10^5$
22	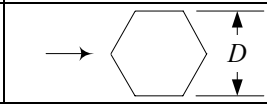	0.156	0.638	$5\times10^4 < \mathrm{Re}_D < 1\times10^6$
23	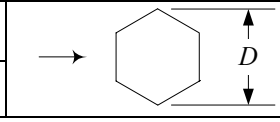	0.163	0.638	$5\times10^4 < \mathrm{Re}_D < 1\times10^6$
24		0.039	0.782	$1.95\times10^5 < \mathrm{Re}_D < 1\times10^6$

X. Closure

In this article, several analytical expressions were derived for k_e. These explicit solutions embody most possible heat pathways and base plate geometries that arise in microelectronic packages. Such approximations are generally valid in industrial applications involving a number of Single and Multiple Chip Packages (SCPs/MCPs), dual in-line packages (DIPs), pin grid arrays (PGAs), plastic leaded chip carriers (PLCCs), leadless ceramic chip carriers (LL-CCCs), ceramic quad packages (CQUADs), and plastic quad packages (PQUADs). From a physical standpoint, the effective thermal conductivity represents a figure-of-merit that assumes an intermediate value greater than that of the coolant ($0.026\ \mathrm{W m^{-1}K^{-1}}$ for air), and smaller than that of the metal ($240\ \mathrm{W m^{-1}K^{-1}}$ for Aluminum, and $400\ \mathrm{W m^{-1}K^{-1}}$ for Copper). In forced convection studies, k_e typically varies between 8 and $16\ \mathrm{W m^{-1}K^{-1}}$. However, it can be smaller than unity under natural convection conditions. In principle, the sole purpose of using a lumped thermal concept has been to provide an expedient approach in modeling populated chip packages. In some research circles, the success of compact models in predicting temperature distributions has made them indispensable to the efficient development of competitive packaging designs. Ultimately, lumped thermal models may be needed not just for compact heat sink representations, but also for other components used in electronic enclosures. These may include combinations of heat sinks and other emerging technologies that are currently underway.

Acknowledgments

The authors wish to thank NASA and the Wisconsin Space Grant Consortium for supporting this work. We are also thankful for the support and encouragement of: Dr. M. Michael Yovanovich at the University of Waterloo, Dr. Yunus A. Çengel at the University of Nevada, and Dr. Lance Collins at Cornell University.

References

[1]Çengel, Y. A., *Heat Transfer: A Practical Approach*, McGraw-Hill, New York, NY, 1998.

[2]Bar-Cohen, A., and Kraus, A. D., *Advances in Thermal Modeling of Electronic Components and Systems*, Vol. 2, ASME Press, New York, NY, 1990.

[3]Kays, W. M., and London, A. L., *Compact Heat Exchangers*, 2nd ed., McGraw-Hill, New York, 1964.

[4]Tuckerman, D. B., and Pease, R. E., "High-Performance Heat Sinking for VLSI," *IEEE Electron Device Letters,* Vol. 2, No. 5, 1981.

[5]Goldberg, N., "Narrow Channel Forced Air Heat Sink," *IEEE Transactions on Components Hybrids and Manufacturing Technology,* Vol. 1, 1984, pp. 154-159.

[6]Sasaki, S., and Kishimoto, T., "Optimal Structure for Microgroove Cooling Fin for High Power LSI Devices," *Electronics Letters,* Vol. 22, No. 25, 1986, pp. 1332-1334.

[7]Hawang, L. T., Turlik, I., and Reisman, A., "A Thermal Module Design for Advanced Packaging," *Journal of Electronic Materials,* Vol. 16, No. 5, 1987, pp. 347-355.

[8]Nayak, D., Hawang, L. T., Turlik, I., and Reisman, A., "A High-Performance Thermal Module for Computer Packaging," *Journal of Electronic Materials,* Vol. 16, No. 5, 1987, pp. 357-364.

[9]Phillips, R. J., "Microchannel Heat Sinks," *Advances in Thermal Modeling of Electronic Components and Systems*, Vol. Chap. 3, Vol. 2, edited by A. Bar-Cohen and A. D. Kraus, ASME Press, New York, NY, 1990.

[10]Gavali, S., Patankar, S. V., Karki, K. C., and Miura, K., "Effect of Heat Sink on Forced Convection Cooling of Electronic Components: A Numerical Study," *Advances in Electronic Packaging,* Vol. 4, No. 2, 1993.

[11]Butterbaugh, M. A., and Kang, S. S., "Effect of Airflow Bypass on the Performance of Heat Sinks in Electronic Cooling," *Advances in Electronic Packaging,* Vol. 10, No. 2, 1995.

[12]Visser, J. A., and Gauche, P., "A Computer Model to Simulate Heat Transfer in Heat Sinks," Proceedings of the Fourth International Conference for Advanced Computational Methods in Heat Transfer, 1996.

[13]Bar-Cohen, A., "Air-Cooled Heat Sinks -Trends and Future Directions," *Advances in Electronic Packaging,* Vol. 19, No. 2, 1997.

[14]Azar, K., McLeod, R. S., and Caron, R. E., "Narrow Channel Heat Sink for Cooling of High Powered Electronic Components," Eighth IEEE SEMI-THERM Symposium, IEEE Service Center, 1992.

[15]Souza Mendes, P. R., and Santos, W. F. N., "Heat-Transfer and Pressure Drop Experiments in Air-Cooled Electronic Component Arrays," *AIAA Journal of Thermophysics and Heat Transfer,* Vol. 1, No. 4, 1987, pp. 373-378.

[16]Vogel, M. R., "Thermal Performance of Air-Cooled Hybrid Heat Sinks for a Low Velocity Environment," Tenth IEEE SEMI-THERM Symposium, IEEE Service Center, 1994.

[17]Wirtz, R. A., Chen, W., and Zhou, R., "Effects of Flow Bypass on the Performance of Longitudinal Fin Heat Sinks," *ASME Journal of Electronic Packaging,* Vol. 116, 1994, pp. 206-211.

[18]Bar-Cohen, A., Elperin, T., and Eliasi, R., "Q_{jc} Characterization of Chip Packages –Justification, Limitations, and Future," *IEEE Transactions on Components Hybrids and Manufacturing Technology,* Vol. 12, No. 4, 1989, pp. 724-731.

[19]Krueger, W., and Bar-Cohen, A., "Thermal Characterization of a PLCC-Expanded Rjc Methodology," *IEEE Transactions on Components Hybrids and Manufacturing Technology,* Vol. 15, No. 5, 1992, pp. 691-698.

[20]Culham, J. R., Yovanovich, M. M., and Lee, S., "Thermal Modeling of Isothermal Cuboids and Rectangular Heat Sinks Cooled by Natural Convection," Concurrent Engineering and Thermal Phenomena Proceedings of the Intersociety Conference on Thermal Phenomena in Electronic Systems, IEEE Service Center, Paper 94CH3340, 1994.

[21]Culham, J. R., Yovanovich, M. M., and Lee, S., "Thermal Modeling of Isothermal Cuboids and Rectangular Heat Sinks Cooled by Natural Convection," *IEEE Transactions on Components Packaging and Manufacturing Technology –Part A,* Vol. 18, No. 3, 1995, pp. 559-566.

[22]Linton, R. L., and Agonafer, D., "Coarse and Detailed CFD Modeling of a Finned Heat Sink," *IEEE Transactions on Components Packaging and Manufacturing Technology –Part A,* Vol. 18, No. 3, 1995, pp. 517-520.

[23]Patel, C. D., and Belady, C. L., "Modeling and Metrology in High Performance Heat Sink Design," IEEE Electronic Components and Technology Conference, IEEE, 1997.

[24]Patel, C. D., and Belady, C. L., *Modeling and Metrology in High Performance Heat Sink Design*, Hewlett Packard Laboratories, Palo Alto, California, 1997.

[25]Kim, S., and Lee, S., "On Heat Sink Measurement and Characterization," The ASME International Electronic Packaging Conference and Exhibition, ASME, Paper INTERPACK'97, 1997.

[26]Narasimhan, S., and Kusha, B., "Characterization and Verification of Compact Heat Sink Models," *Proceedings of the Heat Transfer and Fluid Mechanics Institute*, 1998, pp. 43-46.

[27]Narasimhan, S., and Majdalani, J., "Characterization of Compact Heat Sink Models in Natural Convection," The ASME International Electronic Packaging Conference and Exhibition, IPACK, Paper 2001-15889, July 8-13 2001.

[28]Narasimhan, S., and Majdalani, J., "Characterization of Compact Heat Sink Models in Natural Convection," *IEEE Transactions on Components Packaging and Manufacturing Technology –Part A,* Vol. 25, No. 1, 2002, pp. 78-86.

[29]Andrews, J. A., Mahalingam, M., and Berg, H., "Thermal Characteristics of 16- and 40-Pin Plastic DIPs," *IEEE Transactions on Components Hybrids and Manufacturing Technology,* Vol. 4, 1981, pp. 455-461.

[30]Andrews, J. A., "Package Thermal Resistance Model Dependency on Equipment Design," *IEEE Transactions on Components Hybrids and Manufacturing Technology,* Vol. 11, No. 4, 1988, pp. 528-537.

[31]Mahalingam, M., "Surface-Mount Plastic Packages –an Assessment of Their Thermal Performance," *IEEE Transactions on Components Hybrids and Manufacturing Technology,* Vol. 12, No. 4, 1989, pp. 745-752.

[32]Gautier, "Construction and Validation of Thermal Models of Packages," Seventh IEEE SEMI-THERM Symposium, IEEE Service Center, 1991.

[33]Le Jannou, J. P., and Huon, Y., "Representation of Thermal Behavior of Electronic Components for the Creation of a Databank," *IEEE Transactions on Components Hybrids and Manufacturing Technology,* Vol. 14, No. 2, 1991, pp. 366-373.

[34]Lemczyk, T. F., Culham, J. R., Lee, S., and Yovanovich, M. M., "Fopt – a Thermal Optimization Factor for Microelectronic Packages," Eighth IEEE SEMI-THERM Symposium, IEEE Service Center, 1992.

[35]Lemczyk, T. F., Mack, B. L., Culham, J. R., and Yovanovich, M. M., "PCB Trace Thermal Analysis and Effective Conductivity," *Journal of Electronic Packaging,* Vol. 114, No. 4, 1992, pp. 413-419.

[36]Lasance, C. J. M., Vinke, H., and Rosten, H., "Thermal Characterization of Electronic Devices with Boundary Condition Independent Compact Models," *IEEE Transactions*

on Components Packaging and Manufacturing Technology – Part A, Vol. 18, No. 4, 1995, pp. 723-731.

[37]Narasimhan, S., Bar-Cohen, A., and Nair, R., "Thermal Compact Modeling of Parallel Plate Heat Sinks," *IEEE Transactions on Components Packaging and Manufacturing Technology –Part A*, 2002.

[38]Teertstra, P., Yovanovich, M. M., and Culham, J. R., "Pressure Loss Modeling for Surface Mounted Cuboid-Shaped Packages in Channel Flow," *IEEE Transactions on Components Packaging and Manufacturing Technology –Part A,* Vol. 20, No. 4, 1997, pp. 463-469.

[39]Narasimhan, S., Bar-Cohen, A., and Nair, R., "Flow and Pressure Field Characteristics in the Porous Block Compact Modeling of Parallel Plate Heat Sinks," *IEEE Transactions on Components Packaging and Manufacturing Technology –Part A*, 2002.

[40]Churchill, S. W., and Chu, H. H. S., "Correlating Equations for Laminar and Turbulent Free Convection from a Vertical Plate," *International Journal of Heat and Mass Transfer,* Vol. 18, No. 11, 1975, pp. 1323-1329.

[41]Kraus, A. D., and Bar-Cohen, A., *Thermal Analysis and Control of Electronic Equipment*, Hemisphere, New York, NY, 1983, p. 360.

[42]Churchill, S. W., and Chu, H. H. S., "Correlating Equations for Laminar and Turbulent Free Convection from a Vertical Plate," *International Journal of Heat and Mass Transfer,* Vol. 18, 1975, pp. 1323-1329.

[43]Churchill, S. W., and Churchill, R., U, "A Comprehensive Correlating Equation for Heat an Component Transfer by Free Convection," *AIChE Journal,* Vol. 21, 1975, pp. 604-606.

[44]Cardano, G., *The Rules of Algebra*, edited by T. R. Witmer, Dover, New York, NY, 1993.

[45]McAdams, W. H., *Heat Transmission*, *McGraw-Hill Series in Chemical Engineering*, 3rd ed., edited by S. D. Kirkpatrick, McGraw-Hill Book Company, New York, 1954, p. 532.

[46]Warner, C. Y., and Arpaci, V. S., "An Experimental Investigation of Turbulent Natural Convection in Air at Low Pressure," *International Journal of Heat and Mass Transfer,* Vol. 11, 1968, p. 397.

[47]Eckert, E. R. G., and Jackson, T. W., "Analysis of Turbulent Free Convection Boundary Layer on a Flat Plate," Technical Rept. NACA 1015, NASA, 1951.

[48]Lloyd, J. R., and Moran, W. R., "Natural-Convection Adjacent to Horizontal Surface of Various Planforms," *Journal of Heat Transfer,* Vol. 96, No. 4, 1974, pp. 443-447.

[49]Fujii, T., and Imura, H., "Natural Convection Heat Transfer from a Plate with Arbitrary Inclination," *International Journal of Heat and Mass Transfer,* Vol. 15, No. 4, 1972, pp. 755-767.

[50]Churchill, S. W., "Free Convection around Immersed Bodies," *Heat Exchanger Design Handbook*, edited by K. J. Bell, Hemisphere, Washington, D.C., 1983.

[51]Yovanovich, M. M., "On the Effect of Shape, Aspect Ratio and Orientation Upon Natural Convection from Isothermal Bodies of Complex Shapes," *ASME Heat Transfer Division,* Vol. 82, 1987, pp. 121-129.

[52]Churchill, S. W., and Chu, H. H. S., "Correlating Equations for Laminar and Turbulent Free Convection from a Horizontal Cylinder," *International Journal of Heat and Mass Transfer,* Vol. 18, 1975, pp. 1049-1053.

[53]Morgan, V. T., *The Overall Convective Heat Transfer from Smooth Circular Cylinders*, Vol. 11, Academic Press, New York, NY, 1975.

[54]Al-Arabi, M., and Khamis, M., "Natural Convection Heat Transfer from Inclined Cylinders," *International Journal of Heat and Mass Transfer,* Vol. 25, No. 1, 1982, pp. 3-15.

[55]Oosthuizen, P. H., and Donaldson, E., "Free Convection Heat Transfer from Vertical Cones," *Journal of Heat Transfer,* Vol. 94, 1972, pp. 330-331.

[56]Yuge, T., "Experiments on Heat Transfer from Spheres Including Combined Natural and Forced Convection," *Journal of Heat Transfer,* Vol. 82, 1960, pp. 214-220.

[57]Brucker, K., and Majdalani, J., "Effective Thermal Conductivity for Compact Heat Sink Models Based on the Churchill and Chu Correlation," *IEEE Transactions on Components, Packaging, and Manufacturing Technology – Part A,* Vol. TCPT 2001-135R1, 2002.

[58]Jakob, M., *Heat Transfer*, Vol. 1, John Wiley, New York, 1949.

[59]Whitaker, S., "Forced Convection Heat Transfer Correlations for Flow in Pipes, Past Flat Plates, Single Cylinders, Single Spheres, and for Flow in Packed Beds and Tube Bundles," *AIChE Journal,* Vol. 18, 1972, pp. 361-371.

[60]Eckert, E. R. G., "Engineering Relations for Heat Transfer and Friction in High-Velocity Laminar and Turbulent Boundary Layer Flow over Surfaces with Constant Pressure and Temperature," *Transactions of the American Society of Mechanical Engineers,* Vol. 78, 1956, pp. 1273-1284.

[61]Sogin, H. H., "A Summary of Experiments on Local Heat Transfer from the Rear of Bluff Obstacles to a Lowspeed Airstream," *ASME Journal of Heat Transfer,* Vol. 86, 1964, pp. 200-202.

[62]Tien, K. K., and Sparrow, E. M., "Local Heat Transfer and Fluid Flow Characteristics for Airflow Oblique or Normal to a Square Plate," *International Journal of Heat and Mass Transfer,* Vol. 22, 1979, pp. 349-360.

[63]Sparrow, E. M., and Geiger, G. T., "Local and Average Heat Transfer Characteristics of a Disk Situated Perpendicular to a Uniform Flow," *Journal of Heat Transfer,* Vol. 107, 1985, pp. 321-326.

[64]Wedekind, G. L., "Convective Heat Transfer Measurement Involving Flow Past Stationary Circular Disks," *Journal of Heat Transfer,* Vol. 111, 1989, pp. 1098-1100.